

Gradient-Boosted Generalized Linear Models for Conditional Vine Copulas

David Jobst ^{*}Annette Möller [†]Jürgen Groß [‡]

June 21, 2024

Abstract

Vine copulas are flexible dependence models using bivariate copulas as building blocks. If the parameters of the bivariate copulas in the vine copula depend on covariates, one obtains a conditional vine copula. We propose an extension for the estimation of continuous conditional vine copulas, where the parameters of continuous conditional bivariate copulas are estimated sequentially and separately via gradient-boosting. For this purpose, we link covariates via generalized linear models (GLMs) to Kendall's τ correlation coefficient from which the corresponding copula parameter can be obtained. Consequently, the gradient-boosting algorithm estimates the copula parameters providing a natural covariate selection. In a second step, an additional covariate deselection procedure is applied. The performance of the gradient-boosted conditional vine copulas is illustrated in a simulation study. Linear covariate effects in low- and high-dimensional settings are investigated for the conditional bivariate copulas separately and for conditional vine copulas. Moreover, the gradient-boosted conditional vine copulas are applied to the temporal postprocessing of ensemble weather forecasts in a low-dimensional setting. The results show, that our suggested method is able to outperform the benchmark methods and identifies temporal correlations better. Eventually, we provide an R-package called `boostCopula` for this method.

Keywords: conditional copula; vine copula; dependence modeling; generalized linear models; gradient-boosting; variable selection; ensemble postprocessing.

^{*}Corresponding author, University of Hildesheim, Institute of Mathematics and Applied Informatics, Samelsonplatz 1, 31141 Hildesheim, Germany, jobstd@uni-hildesheim.de

[†]Bielefeld University, Faculty of Business Administration and Economics, Universitätsstraße 25, 33615 Bielefeld, Germany, annette.moeller@uni-bielefeld.de

[‡]University of Hildesheim, Institute of Mathematics and Applied Informatics, Samelsonplatz 1, 31141 Hildesheim, Germany, juergen.gross@uni-hildesheim.de

1 Introduction

In plenty of practical applications, multivariate data needs to be modeled by multivariate statistical models, such as e.g. the multivariate normal distribution. Unfortunately, these models are sometimes too inflexible in their marginal and joint behavior, as they e.g. assume, that all marginal distributions belong to the same family. Copulas allow to overcome this issue, as they model the dependence structure between the variables independently of the univariate marginal distributions.

Often parametric copulas are employed, where the parameters are mostly treated as a constant not related to any covariates. As a natural extension, the copula parameter can depend on covariates which yields to a so-called *conditional copula* originally introduced by Patton (2002). Later, non-parametric (Gijbels et al., 2011; Veraverbeke et al., 2011), semi-parametric (Acar et al., 2010) and Bayesian (Craiu and Sabeti, 2012; Sabeti et al., 2014) formulations of the conditional copula have been investigated. Vatter and Chavez-Demoulin (2015) modeled the copula parameters using generalized additive models (GAMs, Hastie and Tibshirani, 1986; Hastie and Tibshirani, 1990; Wood, 2017). While a two-step approach called inference for margins (IFM, Joe, 1996), where first the marginal distributions and afterwards the conditional copulas are estimated is frequently applied, Klein and Kneib (2015), Radice et al. (2015), and Marra and Radice (2017) estimate the marginal distributions and conditional copula parameters simultaneously.

In particular, if the amount of covariates p becomes large, it is not always straightforward for conditional bivariate copulas to include the most informative and exclude the non-informative covariates. One way to tackle these issues is model-based boosting (Bühlmann and Yu, 2003; Bühlmann and Hothorn, 2007a) which is based on a functional gradient-boosting idea (Friedman, 2001). This approach provides a natural variable selection, shrinks effect estimates leading to a better prediction accuracy, and is robust against multicollinearity issues (Mayr and Hofner, 2018). In a copula regression framework, Hans et al. (2022) developed the so called *boosted copula regression* for continuous bivariate responses in a biomedical context. The parameters of the marginal distributions and the parameter of the copula are estimated jointly using the gradient-boosting approach. Recently, Sanchez et al. (2024) extended this idea for bivariate binary, discrete and mixed responses with application to biomedical data.

However, this boosted copula regression approach comes along with some drawbacks. Most notably, it is restricted to bivariate copulas only. Extending this approach in its current fashion to multivariate copulas might be time-consuming due to the modeling of the marginal distributions and a conditional copula jointly. Furthermore, the zoo of multivariate parametric copulas is limited (Genest et al., 2009) and they usually assume homogeneous dependence among the variables, which would restrict the boosted copula regression in its flexibility for dependence modeling. Additionally, the gradient-boosting generally tends to include too many covariates in a low-dimensional setting, which can lead to a slow overfitting (Hans et al., 2022). Eventually, a larger set of more flexible copula families might be beneficial for different applications.

To overcome these issues, we follow the two-step approach (IFM), where the marginal distributions can be individually individually specified by the user in advance. In the next step a conditional multivariate copula is estimated. Latter is implemented as follows:

- (i) We suggest the use of a *vine copula* as a flexible copula class. A vine copula can be

- obtained by decomposing a copula into a cascade of bivariate copulas and linking the bivariate copulas to a graph theoretical object, called *regular vine* (Aas et al., 2009; Bedford and Cooke, 2001). This allows a more flexible dependence modeling.
- (ii) Similar to Vatter and Chavez-Demoulin (2015) and Vatter and Nagler (2018), we employ conditional bivariate copulas, where the copula parameter is derived from Kendall’s τ to which the covariates are linked in terms of a generalized linear model (GLM, Nelder and Wedderburn, 1972).
 - (iii) We use the gradient-boosting approach based on Bühlmann and Hothorn (2007a) for the conditional bivariate copula estimation. Moreover, we add an additional deselection step based on the attributable risk as a measure of variable importance (Strömer et al., 2021).
 - (iv) To cover lots of possible dependency patterns, we provide besides of the bivariate Gaussian copula also rotation extended versions of the bivariate (survival) Clayton and (survival) Gumbel copula.

In the following, we restrict us to the case of continuous responses, as for discrete or mixed continuous-discrete responses, e.g. adaptations of the copula families need to be made, which is beyond of the scope of this paper. To the best of the authors knowledge, they are the first to combine conditional vine copulas with a gradient-boosting framework to handle low- and high-dimensional covariate settings. Furthermore, as there currently exists no software for a gradient-boosted based conditional vine copula, the authors provide an R-package called `boostCopula` on <https://github.com/jobstdavid/boostCopula>.

The rest of the article is organized as follows: Section 2 briefly introduces vine copulas and the conditional bivariate copulas in the gradient-boosting framework. Additionally, the estimation procedure for conditional vine copula is explained. A large simulation study for conditional vine copulas is conducted in Section 3, where we evaluate the effect estimates, the variable selection and copula family selection process in a low- and high-dimensional covariate setting. In Section 4 we apply our new approach to the multivariate postprocessing of ensemble weather forecasts and present the results. We close with a conclusion and outlook in Section 5.

2 Methodology

2.1 Vine copulas

Following Sklar’s Theorem (Sklar, 1959), the density function f of an absolutely continuous d -dimensional distribution function $F \sim \mathbf{Y} = (Y_1, \dots, Y_d)$ with marginal distributions F_1, \dots, F_d of Y_1, \dots, Y_d and corresponding copula C is given by

$$f(y_1, \dots, y_d) = c(F_1(y_1), \dots, F_d(y_d)) \cdot \prod_{i=1}^d f_i(y_i), \quad (2.1)$$

where f, f_1, \dots, f_d, c are the density functions of F, F_1, \dots, F_d, C respectively. To allow for a more flexible dependence modeling, Bedford and Cooke (2001) and Bedford and Cooke (2002) provided a decomposition of the copula density c in $d(d-1)/2$ bivariate copula densities. As such a decomposition is not unique, it can be structured by a graphical model called *regular vine* (R-vine) which consists of a sequence of linked trees $T_i = (N_i, E_i)$ with node set N_i and edge set E_i for $i = 1, \dots, d-1$, where the edges in one tree become

the nodes of the next one. By identifying each edge $e \in E_i$ in the tree sequence with a bivariate copula density (*pair-copula density*) $c_{a_e, b_e; D_e}$, the vine copula density c can be written as the product of all pair-copula densities

$$c(\mathbf{u}) = \prod_{i=1}^{d-1} \prod_{e \in E_i} c_{a_e, b_e; D_e}(u_{a_e|D_e}, u_{b_e|D_e}; \mathbf{u}_{D_e}), \quad (2.2)$$

where $\mathbf{u} := (u_1, \dots, u_d) \in [0, 1]^d$ is the realization of $\mathbf{U} := (U_1, \dots, U_d) = (F_1(Y_1), \dots, F_d(Y_d))$, $u_{k_e|D_e} := C_{k_e|D_e}(u_{k_e}|\mathbf{u}_{D_e})$ is the conditional distribution of $U_{k_e}|U_{D_e}$ which can be calculated recursively (Joe, 1996) and $\mathbf{u}_{D_e} := (u_l)_{l \in D_e}$ is a sub-vector of \mathbf{u} . A decomposition of a density as in Equation (2.2) is therefore called *pair-copula decomposition* of the joint density c . The set D_e denotes the *conditioning set* and the singletons a_e, b_e are called *conditioned sets*. Consequently, the nodes labeled by $1, \dots, d$ in the first tree T_1 correspond to the variables U_1, \dots, U_d and the edges e labeled as $(a_e, b_e; D_e) = (a_e, b_e)$ stand for the unconditional dependence of variables U_{a_e} and U_{b_e} modeled by the copula density c_{a_e, b_e} . In the subsequent trees the edges labeled as $(a_e, b_e; D_e)$ describe the dependence of U_{a_e} and U_{b_e} conditioned on $\mathbf{U}_{D_e} = \mathbf{u}_{D_e}$ associated to the copula density $c_{a_e, b_e; D_e}$. However, in the theory of vine copulas it is common to agree on the simplifying assumption

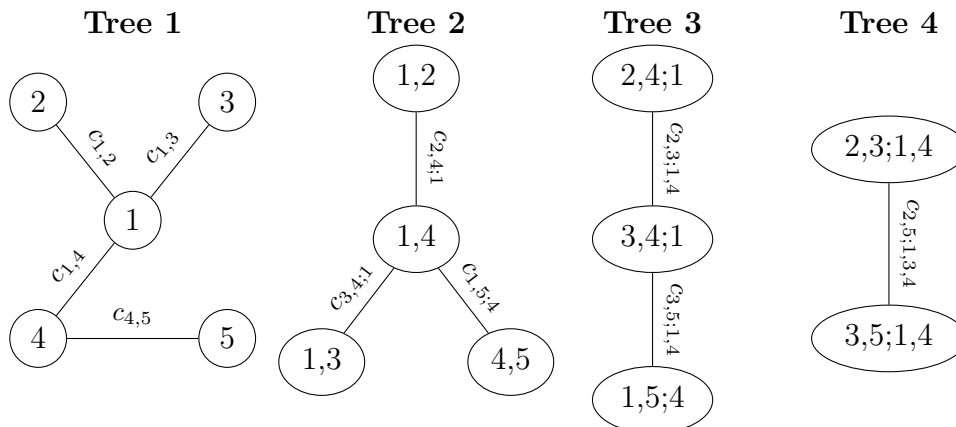


Figure 1: 5-dimensional regular vine and corresponding pair-copula densities.

tion (Stöber et al., 2013) to allow for a tractable estimation of the pair-copula densities. Specifically, this means that we ignore the influence of the variables in the conditioning set \mathbf{u}_{D_e} of the pair-copulas, i.e. $c_{a_e, b_e; D_e}(u_{a_e|D_e}, u_{b_e|D_e}; \mathbf{u}_{D_e}) = c_{a_e, b_e; D_e}(u_{a_e|D_e}, u_{b_e|D_e})$ for all edges e in a regular vine. Consequently, the pair-copula densities $c_{a_e, b_e; D_e}$ describe a partial dependence, rather than a conditional dependence. The conditioning on \mathbf{u}_{D_e} is solely captured by its arguments $u_{a_e|D_e}$ and $u_{b_e|D_e}$. Therefore, the vine copula density in Equation (2.2) simplifies to

$$c(\mathbf{u}) = \prod_{i=1}^{d-1} \prod_{e \in E_i} c_{a_e, b_e; D_e}(u_{a_e|D_e}, u_{b_e|D_e}). \quad (2.3)$$

In Figure 1 a 5-dimensional regular vine is visualized with corresponding (simplified) vine

copula density given by

$$\begin{aligned}
c(u_1, \dots, u_5) &= c_{1,2}(u_1, u_2) \cdot c_{1,3}(u_1, u_3) \cdot c_{1,4}(u_1, u_4) \cdot c_{4,5}(u_4, u_5) && \text{Tree 1} \\
&\cdot c_{2,4;1}(u_{2|1}, u_{4|1}) \cdot c_{3,4;1}(u_{3|1}, u_{4|1}) \cdot c_{1,5;4}(u_{1|4}, u_{5|4}) && \text{Tree 2} \\
&\cdot c_{2,3;1,4}(u_{2|1,4}, u_{3|1,4}) \cdot c_{3,5;1,4}(u_{3|1,4}, u_{5|1,4}) && \text{Tree 3} \\
&\cdot c_{2,5;1,3,4}(u_{2|1,3,4}, u_{5|1,3,4}). && \text{Tree 4}
\end{aligned}$$

2.2 Conditional vine copulas

To obtain a conditional vine copula, the parameters of the bivariate copulas need to depend on covariates $\mathbf{Z} := (Z_0, Z_1, \dots, Z_p)$ with realizations $\mathbf{z} := (z_0, z_1, \dots, z_p) \in \mathbb{R}^{p+1}$, i.e. $c_{a_e, b_e; D_e}(u_{a_e|D_e}, u_{b_e|D_e}; \theta_{a_e, b_e; D_e}(\mathbf{z}))$ where $\theta_{a_e, b_e; D_e}(\mathbf{z}) \in \Theta_{a_e, b_e; D_e}$ denotes the copula parameter depending on \mathbf{z} for edge $e = (a_e, b_e; D_e)$ in the regular vine and $\Theta_{a_e, b_e; D_e}$ is the corresponding parameter space. Consequently, a conditional vine copula density is given by

$$c(\mathbf{u}; \mathbf{z}) = \prod_{i=1}^{d-1} \prod_{e \in E_i} c_{a_e, b_e; D_e}(u_{a_e|D_e}, u_{b_e|D_e}; \theta_{a_e, b_e; D_e}(\mathbf{z})). \quad (2.4)$$

2.3 Gradient-boosted conditional bivariate copulas

In the following, we describe the model setup for the gradient-boosted conditional bivariate copulas densities $c(u_1, u_2; \theta(\mathbf{z}))$, which are the building blocks of the resulting conditional vine copula density, see Equation (2.4). In Section 2.4 we then return to the estimation of the resulting conditional vine copula.

2.3.1 Conditional bivariate copulas

As a bijective transformation $h : (-1, 1) \rightarrow \Theta$ between the Kendall's $\tau \in (-1, 1)$ and a copula parameter $\theta \in \Theta$ with corresponding parameter space $\Theta \subseteq \mathbb{R}$ for common copula families can be derived (see Table 1), we model the Kendall's τ correlation coefficient by covariates. Specifically, we assume a generalized linear model (GLM, [Nelder and Wedderburn, 1972](#)) with linear predictor

$$\eta(\mathbf{z}) := \boldsymbol{\beta} \mathbf{z}^T = \beta_0 z_0 + \beta_1 z_1 + \dots + \beta_p z_p, \quad (2.5)$$

and parameters $\boldsymbol{\beta} := (\beta_0, \beta_1, \dots, \beta_p) \in \mathbb{R}^{p+1}$. Note, that an intercept in the GLM can be obtained by forcing $Z_0 = 1$.

Family	Gaussian	Clayton I, II,	Gumbel I, II
$h : (-1, 1) \rightarrow \Theta \subseteq \mathbb{R}$	$h(t) = \sin\left(\frac{\pi t}{2}\right)$	$h(t) = \frac{2t}{1- t }$	$h(t) = \frac{\text{sign}(t)}{1- t }$

Table 1: Bijective transformations h for the considered copula families.

To ensure the restrictions on the Kendall's τ correlation coefficient of the considered copula families, we use the Fisher transformation $f : \mathbb{R} \rightarrow (-1, 1)$, $f(\eta) := \tanh(\eta)$ to

map the linear predictor η to the range of the Kendall's τ correlation coefficient, where we assume the link to be correctly specified. Summing up, we model a single copula parameter via

$$\theta(\mathbf{z}) := h(f(\eta(\mathbf{z}))), \quad (2.6)$$

where we first transform the linear predictor η via the link function f to the Kendall's τ coefficient range and the result thereof into the copula parameter domain via the bijection h . This approach is in contrast to [Hans et al. \(2022\)](#), who modeled the copula parameter directly. However, the parameterization of Kendall's τ correlation coefficient has a simpler interpretation than a copula parameter, especially when the copula parameters live in different domains.

For each conditional bivariate copula in the conditional vine copula the same set of one-parametric copula families is allowed, from which the best fitting copula family is chosen (see Section 2.3.4). The set of all available copula families contains the Gaussian copula from the Elliptical copula class. However, the occurrence of tail dependence ([McNeil et al., 2005](#)) supports the investigation of copula families being different from Gaussian. Therefore, we additionally consider the Clayton and Gumbel copula from the Archimedean copula class which can capture lower and upper tail-dependence, respectively. We extend the Clayton and Gumbel copula by their 90 degrees counter-clockwise rotations to handle the negative Kendall's τ correlation coefficient as well, via

$$c_{\text{Family I}}(u_1, u_2; \tau) := \begin{cases} c_{\text{Family}}(u_1, u_2; \tau), & \tau \geq 0, \\ c_{\text{Family}}(u_2, 1 - u_1; -\tau), & \tau < 0, \end{cases} \quad (2.7)$$

for $\text{Family} \in \{\text{Clayton}, \text{Gumbel}\}$. To obtain even richer dependence structures, survival copulas for Clayton I and Gumbel I are introduced which are 180 degrees counter-clockwise rotated versions thereof, i.e.

$$c_{\text{Family II}}(u_1, u_2; \tau) := c_{\text{Family I}}(1 - u_1, 1 - u_2; \tau), \quad (2.8)$$

for $\text{Family} \in \{\text{Clayton}, \text{Gumbel}\}$. This yields in total the 5 different copula families Gaussian, Gumbel I, Gumbel II, Clayton I, Clayton II visualized in Figure 2 from which the best fitting one can be chosen. Note, that we are actually able to cover 9 different copula families by estimating only the previously mentioned 5 copula families which saves computational resources, too.

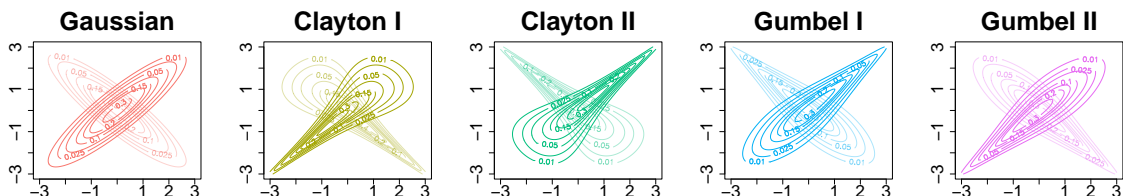


Figure 2: Density contour plots of the Gaussian, Clayton I, Clayton II, Gumbel I, Gumbel II copula for $\tau = 0.7$ (dark) and $\tau = -0.7$ (bright).

2.3.2 Estimation via gradient-boosting

The estimation of the linear predictor η corresponding to the conditional bivariate copulas is based on a gradient-boosting approach. For a pair of standard uniformly distributed random variables (U_1, U_2) with realization $(u_1, u_2) \in [0, 1]^2$ the associated optimization problem can be written as

$$\hat{\eta}_\theta = \arg \min_{\eta} \mathbb{E}_{U_1, U_2 | \mathbf{Z}}[\ell(U_1, U_2; \eta(\mathbf{Z}))], \quad (2.9)$$

where ℓ denotes the loss function. In case of a data set with N observations, the (conditional) expectation $\mathbb{E}_{U_1, U_2 | \mathbf{Z}}$ is replaced by the empirical risk

$$\frac{1}{N} \sum_{i=1}^N \ell(u_1^{(i)}, u_2^{(i)}; \eta(\mathbf{z}^{(i)})), \quad (2.10)$$

measuring how well the (transformed) linear predictor fits the Kendall's τ correlation coefficient inherent in the copula data. Furthermore, we select the negative log-likelihood of the conditional bivariate copula density as loss function ℓ .

Algorithm 1 Gradient-boosting

Initialization Initialize $(\beta_0^{[0]}, \beta_1^{[0]}, \dots, \beta_p^{[0]}) := (0, \dots, 0)$.

Boosting For each iteration $m = 1, \dots, m_{\text{stop}}$:

1. Calculate the negative gradient $\mathbf{g} \in \mathbb{R}^N$ of the loss function:

$$\mathbf{g} := (g^{(i)})_{i=1, \dots, N} := - \left(\frac{\partial}{\partial \eta} \ell(u_1^{(i)}, u_2^{(i)}; \eta^{[m-1]}(\mathbf{z}^{(i)})) \right)_{i=1, \dots, N}.$$

2. Fit for each covariate a separate linear regression model without intercept in the sense of ordinary least squares to the negative gradient:

$$g^{(i)}(z_j^{(i)}) = \hat{\beta}_j z_j^{(i)}, \quad i = 1, \dots, N,$$

with slope $\hat{\beta}_j \in \mathbb{R}$ for each covariate Z_j , $j = 0, 1, \dots, p$.

3. Select the index j^* which minimizes the residual sum of squares criterion:

$$j^* := \arg \min_{j=0, 1, \dots, p} \sum_{i=1}^N (g^{(i)} - \hat{\beta}_j z_j^{(i)})^2.$$

4. Update the current estimate by

$$\beta_{j^*}^{[m]} = \beta_{j^*}^{[m-1]} + \nu \cdot \hat{\beta}_{j^*}, \quad \beta_j^{[m]} = \beta_j^{[m-1]}, \quad j \in \{0, 1, \dots, p\} \setminus \{j^*\},$$

using step length $\nu \in (0, 1]$.

Finalization Set $(\beta_0, \beta_1, \dots, \beta_p) := (\beta_0^{[m_{\text{stop}}]}, \beta_1^{[m_{\text{stop}}]}, \dots, \beta_p^{[m_{\text{stop}}]})$.

The basic idea of gradient-boosting is to minimize the empirical risk by a stepwise gradient-descent of the loss function. The procedure (Bühlmann and Yu, 2003; Bühlmann and Hothorn, 2007a) is summarized in Algorithm 1. Consequently, due to the selection of

a single covariate and the update of the corresponding coefficient (step 3. and 4. of Algorithm 1) in each iteration, the algorithm performs a variable selection. This procedure is carried out until a maximum number of iterations m_{stop} is reached (Hofner et al., 2012). The maximum number of boosting iterations m_{stop} is an important tuning parameter for the gradient-boosting procedure as it helps to prevent overfitting and supports the sparsity of the final model by a data-driven variable selection and yields to an improved prediction accuracy (Hofner et al., 2012). It is usually selected by cross-validation (CV) or AIC minimization. Another tuning parameter is the step length ν for which a small value of e.g. $\nu = 0.1$ has been established as appropriate in most cases (Hofner et al., 2012).

2.3.3 Deselection of covariates

Especially for low-dimensional settings, the gradient-boosting algorithm in Section 2.3.2 tends to include too many covariates, which results in a slow overfitting. To overcome this issue and to achieve sparse models, we follow Strömer et al. (2021) and apply a deselection procedure for the covariates after the gradient-boosted estimation of the conditional bivariate copula. In a subsequent step, we boost the conditional bivariate copula again only with the remaining covariates from the deselection procedure using the already previously determined optimal number of boosting iterations m_{opt} (by cross-validation or AIC minimization). For the deselection step, the attributable risk reduction

$$R_j := \sum_{m=1}^{m_{\text{stop}}} \mathbb{1} \{j = j^{*[m]}\} \cdot (r^{[m-1]} - r^{[m]}), \quad j = 0, 1, \dots, p, \quad (2.11)$$

is considered as a measure for variable importance of the j -th covariate Z_j .

Algorithm 2 Gradient-boosting with additional deselection of covariates

- 1. Initial boosting:** Estimate the conditional bivariate copula via gradient-boosting with an initial number of boosting iterations m_{stop} .
 - 2. Early stopping:** Tune the optimal number of boosting iterations m_{opt} via cross-validation or AIC minimization.
 - 3. Deselection of covariates:** Deselect the covariates with the smallest impact on the risk reduction according to Equation (2.12).
 - 4. Final boosting:** Boost the conditional bivariate copula again with the remaining covariates of step 3. and m_{opt} of step 2.
-

Here, $\mathbb{1}$ denotes the indicator function, $j^{*[m]}$ corresponds to the selected covariate $Z_{j^{*[m]}}$ of the initial boosting and $r^{[m-1]} - r^{[m]}$ gives the risk reduction at iteration m for the risk $r^{[m]}$ at iteration m and the risk $r^{[m-1]}$ at iteration $m - 1$. The risk is given by the value of loss function ℓ , i.e. in our case the negative log-likelihood. Consequently, the j -th covariate Z_j is deselected if

$$R_j < \gamma \cdot (r^{[0]} - r^{[m_{\text{stop}}]}), \quad (2.12)$$

for a given threshold $\gamma \in (0, 1)$, where $r^{[0]} - r^{[m_{\text{stop}}]}$ is the total risk reduction. Consequently, only covariates for which the relative risk contribution is greater than or equal to

the threshold γ will be kept in the model. [Strömer et al. \(2021\)](#) suggest the use of a small threshold, e.g. $\gamma = 0.01$, but also outline, that the choice of γ depends on the research situation. Therefore, the selection of γ is a trade-off between more complex models with higher prediction accuracy and sparser, more interpretable models with possibly lower prediction performance ([Strömer et al., 2021](#)). Summing up, for a specified copula family the conditional bivariate copula is estimated in the four steps described in Algorithm 2.

2.3.4 Copula family selection

After having estimated a specified subset of copulas from the set of 5 copula families via Algorithm 2, the copula family can be selected by goodness-of-fit measures, for example log-likelihood or complexity criteria, such as Akaike information criterion (AIC, [Akaike, 1998](#)). As the gradient-boosting results in regularized model fits, the model complexity can be hard to evaluate ([Hastie, 2007](#)). Therefore, [Hofner et al. \(2016\)](#) suggest to use the predictive empirical risk, i.e. the evaluation of the negative log-likelihood on a new data set (out-of-sample). [Hans et al. \(2022\)](#) employ this measure to decide which copula family should be chosen. Unfortunately, this comes with the drawback of a reduction in the size of the training data, which can lead to a loss in the prediction accuracy for the copula parameter. Furthermore, it might yield to a biased copula family selection, especially, when the training data size is not large. However, in the copula theory, the AIC is frequently applied for the copula family selection, as it has proven to be a reliable selection criterion ([Brechmann, 2010](#)). Therefore, we investigate the AIC as copula selection criterion, where we approximately determine the degrees of freedom based on the number of nonzero coefficients (active set) in Equation (2.5). According to [Bühlmann and Hothorn \(2007b\)](#), the active set can work reasonable well as measure for the model degrees of freedom.

2.4 Estimation of conditional vine copulas

Until now, we have only introduced the estimation and selection of conditional bivariate copulas. In the following, we briefly describe the corresponding estimation procedure for a d -dimensional conditional vine copula with predetermined regular vine.

We use a sequential top-down estimation ([Aas et al., 2009](#); [Czado, 2019](#)) for the conditional bivariate copulas in a conditional vine copula, where the conditional bivariate copulas are separately estimated via Algorithm 2 for the allowed set of copula families for each edge in tree T_1 . Then, the copula family is selected as described in Section 2.3.4 for each edge in tree T_1 . Afterwards this estimation and selection procedure of the conditional bivariate copulas is applied to the remaining trees T_j , $j = 2, \dots, d - 1$. While the copula data $\mathbf{u} = (u_1, \dots, u_d)$ for the first tree T_1 is given, the copula data for the higher trees T_j with $j = 2, \dots, d - 1$ is unobserved. However, so-called *pseudo-observations* calculated based on the recursion formula in [Joe \(1996\)](#) can be used as copula data in the higher trees. Note that a regular vine might not always be given in advance and therefore needs to be estimated. However, as we do not consider this setting throughout the article, we refer to [Dißmann et al. \(2013\)](#) and [Czado \(2019\)](#) for more details. Nonetheless, the regular vine estimation based on [Dißmann et al. \(2013\)](#) does not represent any obstacle for our suggested estimation procedure and is therefore implemented in the R-package `boostCopula` as well.

3 Simulations

In this section, we would like to analyze the properties of the gradient-boosted conditional vine copulas for low- and high-dimensional covariate settings. Similar to [Sanchez et al. \(2024\)](#), we carry out a simulation study where we first generate samples (Z_1, \dots, Z_{p-1}) from a multivariate normal distribution $\mathcal{N}_{p-1}(0, \Sigma)$ with Toeplitz covariance matrix $\Sigma_{ij} = \rho^{|i-j|}$ for $1 \leq i, j \leq p-1$, correlation $\rho \in (0, 1)$ and sample size N . Specifically, we consider two low-dimensional ($N = 1000, p = 101$; $N = 2000, p = 501$) and two high-dimensional ($N = 1000, p = 2001$; $N = 2000, p = 4001$) scenarios each in a low-correlated $\rho = 0.2$ and high-correlated $\rho = 0.8$ setting. For each case we perform $n = 100$ simulation runs, where we assume for a standardized validation across all conditional bivariate copulas the linear predictor

$$\eta(\mathbf{z}) := 0.1z_0 - 0.2z_1 + 0.3z_2 + 0.2z_3 + 0.5z_4 - 0.4z_5, \quad (3.1)$$

with intercept $Z_0 = 1$, meaning that the covariates Z_0, Z_1, \dots, Z_5 are part of the true data generating process and thus informative, while the covariates Z_6, \dots, Z_{p-1} are not used to generate the data, and thus can be considered as non-informative covariates. Afterwards, we generate samples from the conditional bivariate copula for a fixed copula family. For the estimation of the conditional bivariate copula we apply Algorithm 2 with maximum number of boosting iterations $m_{\text{stop}} = 500$ and the commonly suggested specifications for the step length $\nu = 0.1$ and the deselection threshold $\gamma = 0.01$.

In Section 3.1 we investigate the estimation and selection of all available 5 copula families (Gaussian, Gumbel I, Gumbel II, Clayton I, Clayton II) separately. In Section 3.2 we examine the gradient-boosted estimation and selection of the conditional bivariate copulas for conditional vine copulas as described in Section 2.4. Eventually, we would like to answer the following questions for Algorithm 2 by this simulation study:

1. How well does Algorithm 2 estimate the coefficients for the informative covariates?
2. Is Algorithm 2 able to select the informative and deselect the non-informative covariates?
3. Are the specified copula families reasonably well selected according to AIC?
4. Does AIC work sufficiently well as early stopping criterion in comparison to CV?
5. How do the results of questions 1.-3. look like for a conditional vine copula depending on the tree level?

For the simulation study and the application in Section 4 we use the software R ([R Core Team, 2020](#)), running version 3.6.3 and the R-package `boostCopula`. Additionally, we run our codes on a cluster where we access 10 cores for code parallelization on each node.

3.1 Conditional bivariate copulas

In this section, we investigate the estimation and selection of the five copula families Gaussian, Gumbel I, Gumbel II, Clayton I, Clayton II for low- and high-correlated covariates in low- and high-dimensional settings. We compare the AIC and CV as stopping criteria as well analyze the performance of the AIC for the copula family selection.

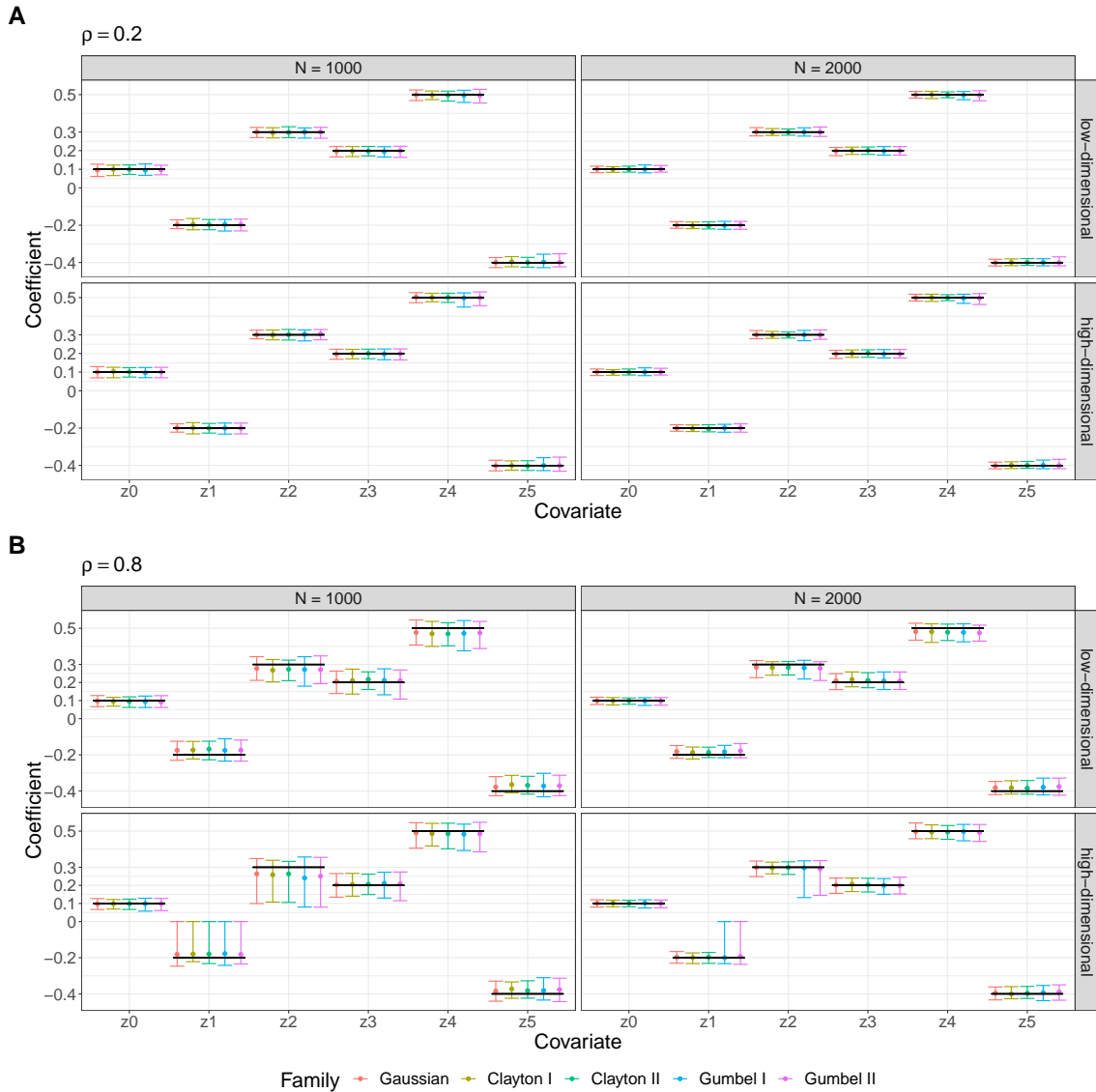


Figure 3: Summary of estimated coefficients with AIC as stopping criterion, where the bars represent the range from the 5% to the 95% quantiles and the points denote the median of the estimated coefficients for the low-correlated (A) and high-correlated (B) setting. The color represent the copula families. The horizontal black lines correspond to the true coefficients.

Parameter estimation. Figure 3 presents the accuracy of the estimated coefficients for the informative covariates represented by the black lines of all considered copula families with AIC as stopping criterion. Firstly, we cannot observe large differences in the median coefficient estimates across the different copula families in all settings. Secondly, Algorithm 2 estimates the coefficients with less bias and variance in the low-correlated ($\rho = 0.2$) setting, while both of these properties become more pronounced for the high-correlated ($\rho = 0.8$) setting. Furthermore, we can observe, that increasing the sample size from $N = 1000$ to $N = 2000$ yields to sharper and less biased coefficients independently

of the correlation setting or covariate dimension. Eventually, Table 2 shows, that the AIC stopping criterion yields coefficient estimates which are in median closer to the true coefficients in contrast to the CV stopping criterion.

Dimension	Stopping criterion	$\beta_0 = 0.1$	$\beta_1 = -0.2$	$\beta_2 = 0.3$	$\beta_3 = 0.2$	$\beta_4 = 0.5$	$\beta_5 = -0.4$
low-dimensional	AIC	0.098	-0.191	0.292	0.202	0.492	-0.392
	CV	0.093	-0.180	0.282	0.200	0.482	-0.380
high-dimensional	AIC	0.100	-0.197	0.297	0.201	0.497	-0.396
	CV	0.088	-0.166	0.270	0.198	0.471	-0.366

Table 2: Medians of the estimated coefficients $\hat{\beta}_0, \dots, \hat{\beta}_5$ for the informative covariates over all copula families, correlation settings $\rho \in \{0.2, 0.8\}$ and sample sizes $N \in \{1000, 2000\}$.

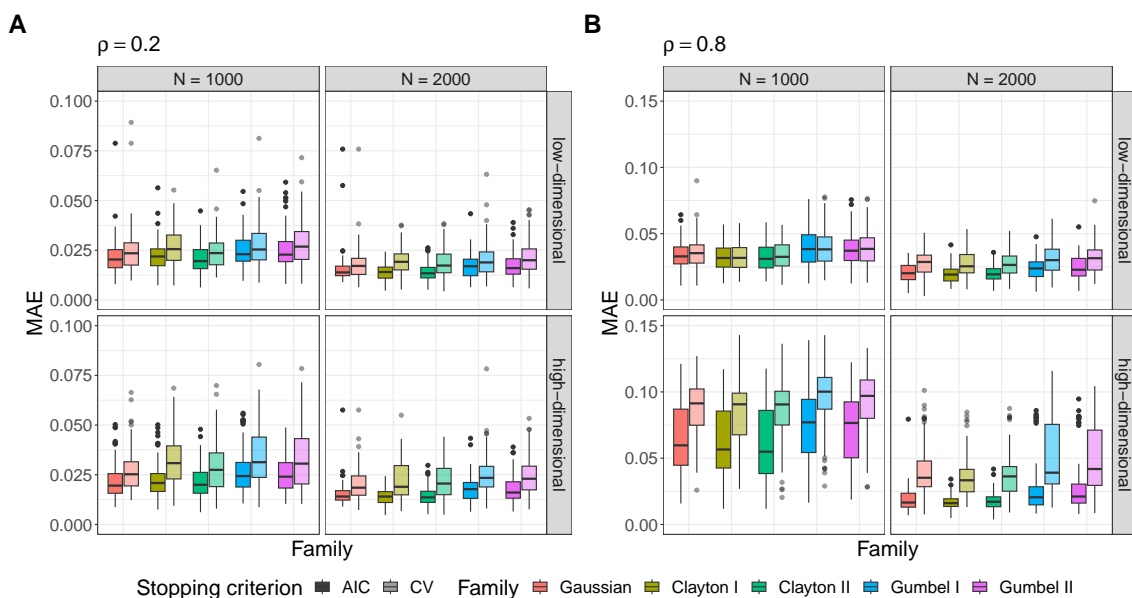


Figure 4: Boxplots of the mean absolute error (MAE) of Kendall's τ correlation coefficient for the low-correlated (A) and high-correlated (B) setting. The color represent the copula families while the color transparency indicates the stopping criterion.

Latter observation is further illustrated in Figure 4, presenting the boxplots of the *mean absolute errors*

$$\text{MAE} := \frac{1}{N} \sum_{i=1}^N |h(f(\eta(\mathbf{z}^{(i)}))) - h(f(\hat{\eta}(\mathbf{z}^{(i)})))|, \quad (3.2)$$

for Kendall's τ correlation coefficient. Note, that one outlier (0.177) in the high-dimensional setting $N = 1000$, $\rho = 0.2$ for the Clayton II family using stopping criterion CV is not displayed for a better boxplot representation. The AIC stopping criterion yields in median to lower values for MAE than CV and increasing the sample size also helps to reduce the MAE in general. One reason for the superiority of AIC over CV is that

AIC tends to stop a bit later than CV for the optimal number of boosting iterations m_{opt} (see Appendix A), which allows more optimization iterations for the coefficients after the deselection procedure than the earlier stopping CV. Furthermore, we can mostly detect no large differences among the copula families but observe slightly higher MAE values in the high-correlated than in the low-correlated setting. Overall, these results are in line with the ones of Figure 3 and Table 2.

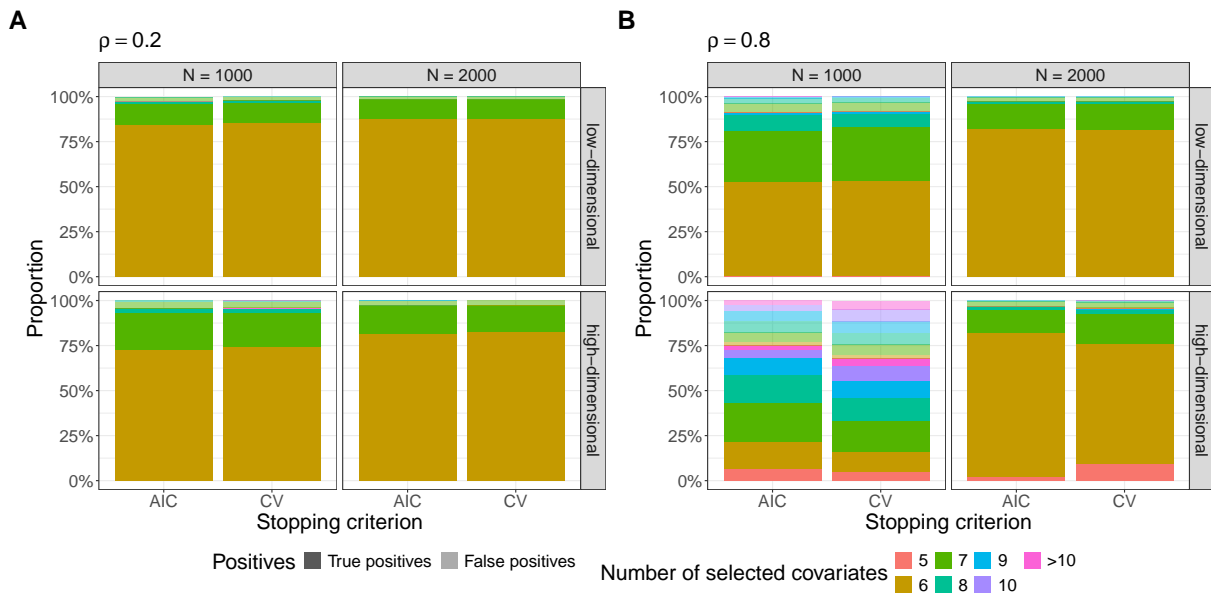


Figure 5: Bar charts for proportion of selected covariates across all 5 copula families and $n = 100$ repetitions. The color transparency represents the proportion of true (dark) and false (light) positives for each number of selected covariates in the stacked bar charts.

Covariate selection. As one might expect already from the previous results, there have been no strong differences among the copula families with respect to the covariate selection, and therefore we have a look at the covariate selection across all copula families in Figure 5. The color transparency represents the proportion of true (dark) and false (light) positives for each number of selected covariates, while the sum of both proportions yield the total proportion for the selected number of covariates. In nearly each setting, six covariates are most frequently selected, followed by seven selected covariates. Furthermore, we observe that Algorithm 2 selects in over 70% of all cases only the six truly informative covariates, except in the high-correlated settings with sample size $N = 1000$. Especially in the high-correlated setting, we observe that increasing the sample size $N = 2000$ yields to a strong improvement in the sense of favouring the selection of all six informative covariates, reducing the spread in the number of selected covariates at the same time. With regard to the stopping criterion and proportion of true and false positives we can say, that there are no strong differences. With respect to the false positives, we deduce that its proportion compared to the true positives is rather small in all scenarios besides of the high-correlated, high-dimensional setting with sample size $N = 1000$.

Copula family selection. As there are no strong differences among the low- and high-correlated setting, Figure 6 shows the percentage of false selected copula families based on the AIC over all $n = 100$ repetitions for both correlation settings. Firstly, the Gaussian, Clayton I, II families are identified overall the best, while instead of the Gumbel I, II families, other families are more often chosen. Depending on the given configuration, either AIC or CV as stopping criterion yields slightly higher selection rates for the underlying copula family, while increasing the sample size shows only strong effect on the selection rate for the high-dimensional configuration. Moreover, we conclude that the AIC works reasonably well in any of these settings to identify the true copula family. In comparison to other copula family selection criteria, e.g. (in-sample) log-likelihood or predictive risk we found that AIC performs comparable or sometimes even better (see Appendix A).

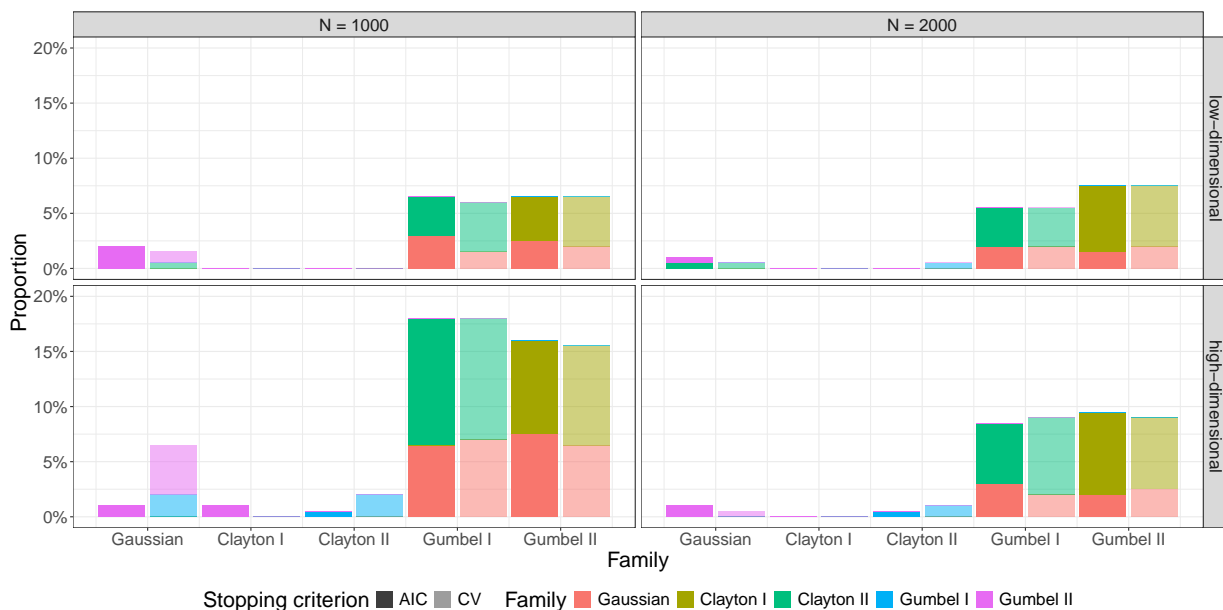


Figure 6: Percentage of false selected copula families for each specified copula family based on the AIC aggregated over the low-correlated and high-correlated setting. The colors represent the copula families while the color transparency indicates the stopping criterion.

To sum up, we conclude that AIC is able to outperform CV as stopping criterion with respect to model accuracy, and it additionally provides a strong improvement with respect to the average computation times (see Appendix A). Furthermore, the AIC is suitable to identify the true copula family. Therefore, we suggest to estimate the considered conditional bivariate copula families with AIC as stopping criterion and use the AIC as copula family selection criterion.

3.2 Conditional vine copula

Similar to [Vatter and Nagler \(2018\)](#), we choose a 5-dimensional vine copula as specified in Figure 1. The copula family for each pair-copula is randomly drawn from the available 5 copula families with equal probability. In a first scenario, called “Selected” model,

the conditional bivariate copulas are estimated and selected as described in Section 2.4 with the sequential top-down estimation procedure. We apply Algorithm 2 with AIC as stopping criterion and the AIC as copula family selection criterion, as it was found to work well in Section 3.1. In a second scenario, called “Specified” model, we only estimate the conditional bivariate copulas via gradient-boosting, while the copula families have already been selected. Additionally, only the informative covariates are included for the GLM and estimated via Algorithm 1 without any covariate deselection afterwards. Latter setting serves as benchmark model to outline, how Algorithm 1 performs under a correct model specification in contrast to the “Selected” model setting. For both scenarios we choose the same tuning parameters as in Section 3.1.

Parameter estimation. Figure 7 presents the accuracy of the estimated coefficients for the six informative covariates in each tree level. Independent of the considered setting, we observe that the true effects are estimated quite well in median for the first two tree levels, while the coefficients become biased towards a value of zero for tree level 3 and 4. This shrinkage towards zero has already been discovered for conditional vine copulas by [Vatter and Nagler \(2018\)](#), who determined the (penalized) maximum-likelihood coefficient estimates of the conditional bivariate copula employing a generalized ridge regression approach. Further investigations outlined that the Algorithm of [Vatter and Nagler \(2018\)](#) showed a similar shrinkage towards zero for the coefficients in our simulation settings, even though this effect was not as pronounced as for the gradient-boosted based estimation (see Appendix B). The bias towards zero in the coefficients for increasing tree levels is a result of the sequential estimation procedure, as the estimation errors in the current tree reproduce and hide the covariate effects in the subsequent trees. Although this shrinkage was not intended, it might motivate to specify even more parsimonious models with less parameters, e.g. by truncating the regular vine at a certain tree level.

Furthermore, we observe that the median coefficient estimates of the “Specified” models are a bit closer to the true coefficients in contrast to the “Selected” models. Additionally, increasing the sample size helps again to reduce the bias in the coefficient estimates.

Figure 8 shows boxplots of the mean absolute error (MAE) of Kendall’s τ correlation coefficient. We observe that the MAE becomes in general larger with increasing tree level, for each of the considered settings, which underlines our previous findings. While the median MAE is generally lower for the low-correlated setting in tree levels 1 and 2, the models in the high-correlated setting perform better with respect to the same measure in tree levels 3 and 4. Furthermore, there are no strong differences among the selected and specified model in terms of the median MAE, but we observe a large amount of outliers with high values for the specified model in each tree and simulation setting. These outliers can be traced back to the cases, where Algorithm 1 selects in total only very few covariates, meaning specifically, a small number of the informative covariates (mostly one or two, see Appendix B) for the “Specified” models. In contrast, Algorithm 2 chooses additional non-informative covariates in these situations, which leads to an overfitting for the “Selected” models, but lower MAE. Eventually, increasing the sample size reduces the MAE independently of the simulation setting.

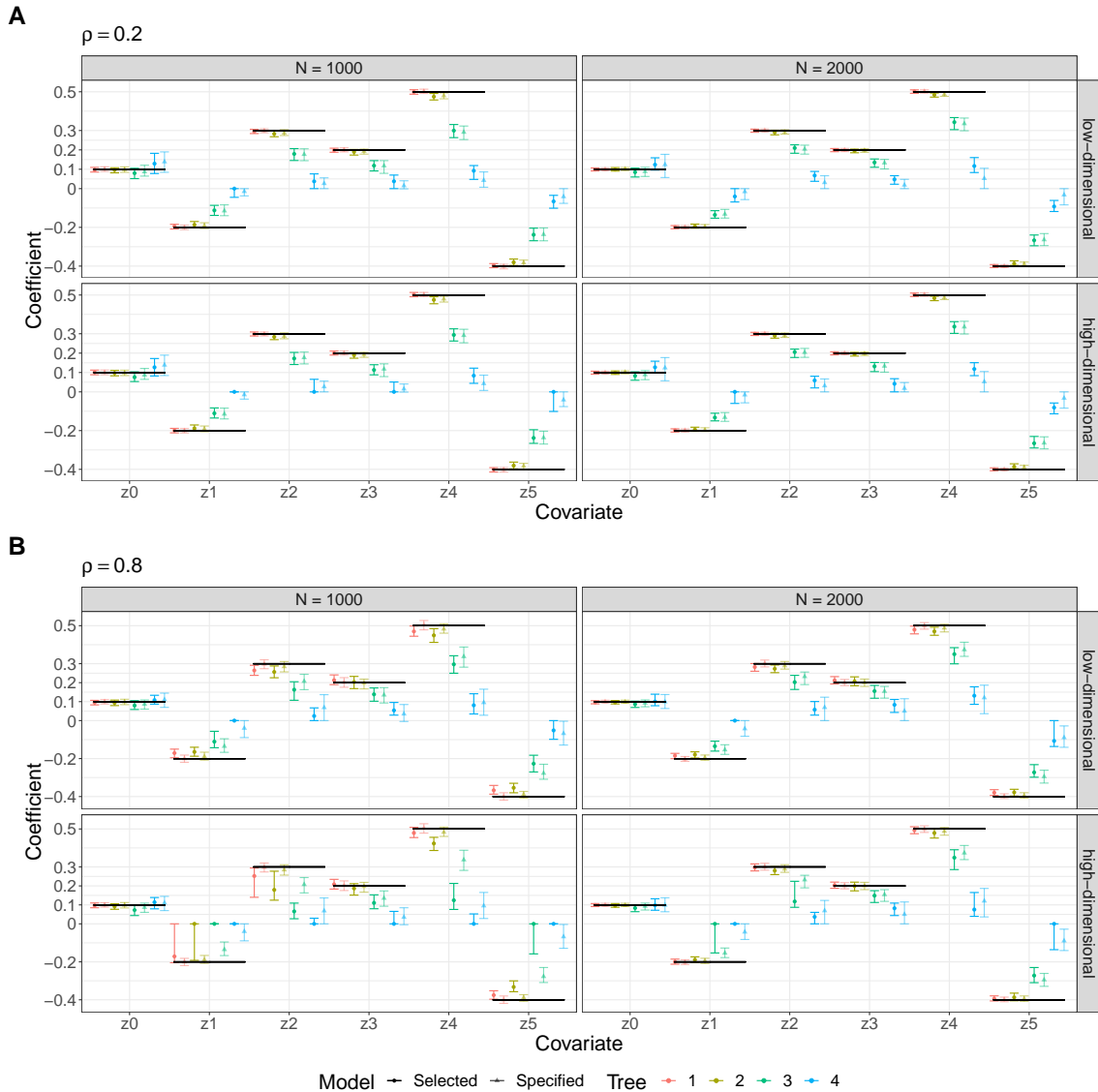


Figure 7: Summary of estimated coefficients, where the error bars represent the interquartile range and the points denote the median of the estimated coefficients for the low-correlated (A) and high-correlated (B) setting. The horizontal black lines correspond to the true coefficients. The colors represent the tree level while the color transparency indicates the copula model.

Covariate selection. In Figure 9, the color transparency represents the proportion of true (dark) and false (light) positives for each number of selected covariates. Both values together yield the total proportion for each occurring number of selected covariates across all copulas in each tree level. For tree levels 1, 2, we observe that 6 or 7 covariates are most frequently selected, where an increased sample size helps to enhance the proportion of six selected informative covariates. Furthermore, the proportion of true positives is much higher than the proportion of false positives for the cases where 6 or 7 covariates are selected. Therefore we deduce that with increasing sample size it gets more likely,

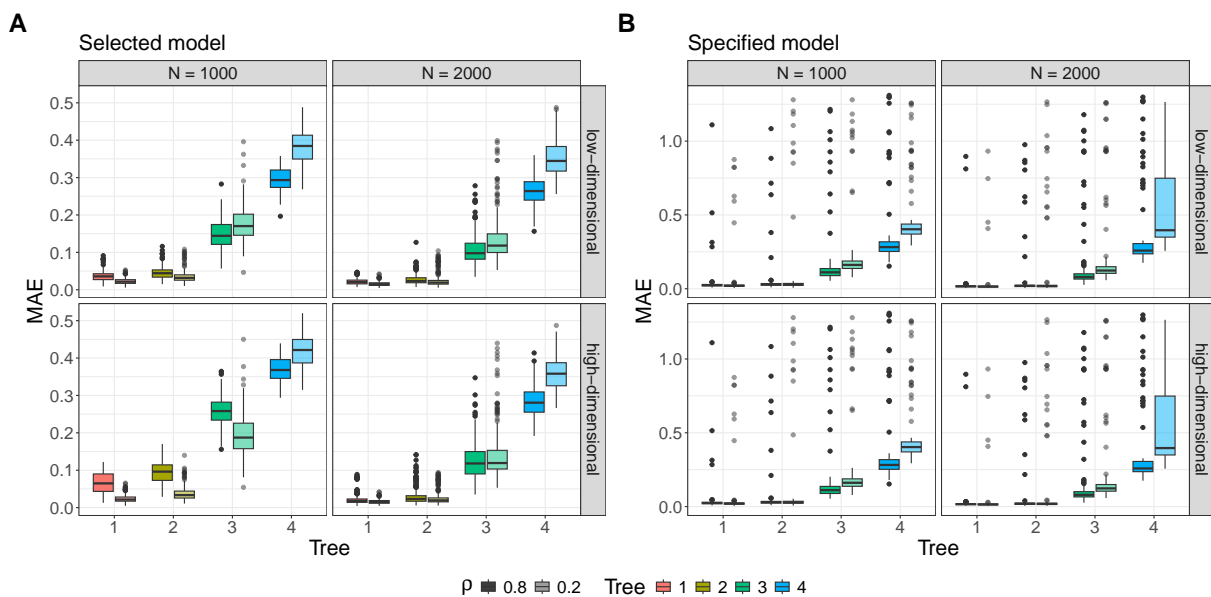


Figure 8: Boxplots of the mean absolute error (MAE) of Kendall's τ correlation coefficient for the selected (A) and specified (B) model. The colors represent the tree level while the color transparency stands for correlation ρ .

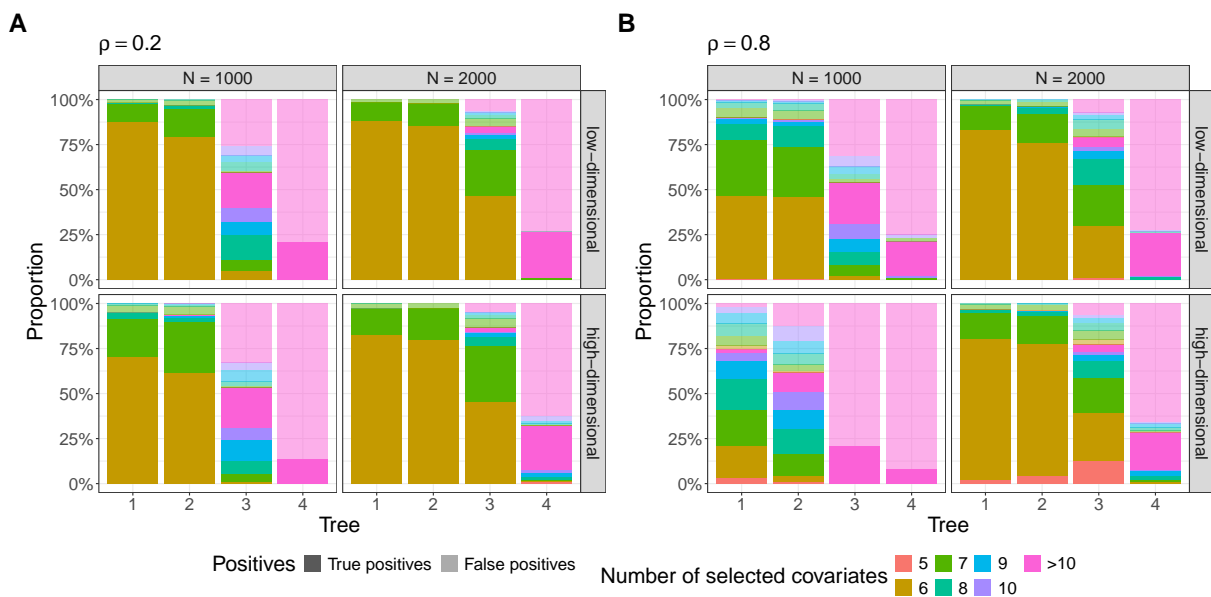


Figure 9: Bar charts for the proportion (%) of selected covariates across all copulas for each tree level and $n = 100$ repetitions in the "Selected" model for the low-correlated (A) and high-correlated (B) setting. The color transparency represents the proportion of true (dark) and false (light) positives for each number of selected covariates in the stacked bar charts.

that all informative covariates are included in tree levels 1, 2 for the conditional bivariate copulas in the cases where 6 or 7 covariates are selected. With increasing tree level, there is a reduction in the proportion of cases where a moderate number (especially 6 or 7) of covariates is selected, while the proportion of cases where 8, 9, 10 or more than 10 covariates are selected clearly increases. For tree level 4, we observe that usually more than 10 covariates are selected. Furthermore, the proportion of false positives in comparison to true positives is clearly higher in tree level 4. In terms of the correlation setting, we only detect large differences in the proportion of cases for the numbers of selected covariates for the smaller sample size.

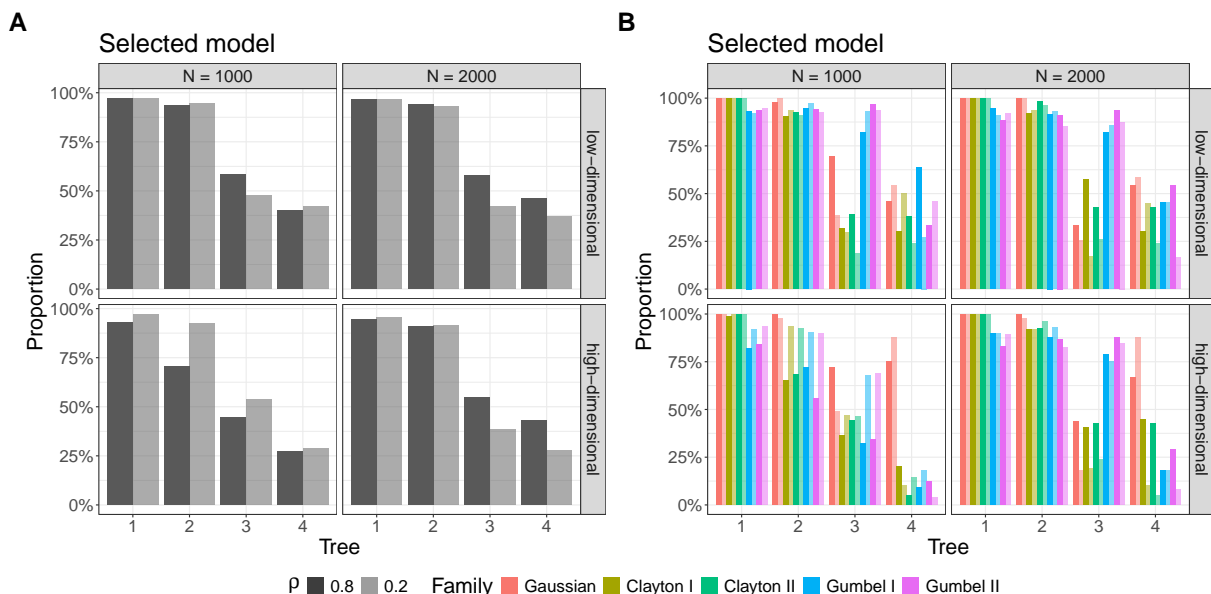


Figure 10: Percentage of correctly selected copula families aggregated over all 5 copula families (A) and for a specified copula family (B). The color represent the copula family while the color transparency stands for correlation ρ .

Copula family selection. Figure 10 shows the percentage of correctly selected copula families aggregated over all 5 copula families (A) and for a specified copula family (B) at each tree level. Again, we observe in (A) that the estimation errors influence the model fit, as the true copula families are selected mostly correct for the first two tree levels and then the selection rate drops for tree levels 3 and 4. As one might already expect, larger samples sizes tend to guarantee a higher percentage for the selection of the true copula family. However, we can detect no obvious trend in the selection rate across the copula families in (B).

All in all, we conclude that the gradient-boosting including a covariate deselection mechanism (Algorithm 2) selects the informative covariates and estimates its corresponding coefficients quite well for lower tree levels independently of the covariate dimension. Furthermore, the AIC copula family selection criterion selected the true copula family quite accurate in the lower tree levels, with increasing bias in the subsequent trees. In the following section, we additionally demonstrate the benefits of the gradient-boosted con-

ditional vine copulas for temperature forecasting in a low-dimensional covariate setting with 15 covariates.

4 Application to temperature forecasting

Weather forecasting is currently based on numerical weather prediction systems (NWP), creating an ensemble of weather forecasts, to quantify the forecast uncertainty. As these forecasts suffer from systematic biases and dispersion errors, they may benefit from statistical postprocessing (Vannitsem et al., 2018). For postprocessing of univariate weather quantities, various statistical methods have been suggested, as, e.g., ensemble model output statistics (EMOS, Gneiting et al., 2005). However, statistical independence among the univariate postprocessed marginal distributions of different lead times is sometimes implicitly assumed. This assumption, is often too restrictive and might cause incoherence. Therefore, the corresponding temporal dependence (Pinson and Girard, 2012; Lakatos et al., 2023) should be restored after the univariate postprocessing to obtain consistent forecasts.

In the following case study, we focus on restoring temporal dependencies for 2 m surface temperature forecasts of five different lead times at a single weather station. After a short description of the data set, we present the univariate and multivariate postprocessing methods. We follow the IFM approach, where we first postprocess the temperature forecasts for each lead time separately via EMOS. In a second step, we restore the (temporal) dependence among the lead times by copula approaches to obtain coherent forecasts. Specifically, we compare the Gaussian copula approach (Möller et al., 2013) and the ensemble copula coupling (Scheffzik et al., 2013) with the gradient-boosted conditional vine copulas. Afterwards, we present the results of the copula based approaches in terms of forecast skill and estimated effects.

4.1 Data

The 2 m surface temperature forecasts obtained from the [European Centre for Medium-Range Weather Forecasts \(ECMWF\) \(2021\)](#) consist of 50 perturbed ensemble forecasts for each of the five lead times 24 h, 48 h, 72 h, 96 h, 120 h. The forecasts have been initialized at 1200 UTC, have a spatial grid resolution of $25^\circ \times 25^\circ$ (≈ 28 km squared) and are bilinearly interpolated to the spatial coordinates of the city Munich in Germany. The [DWD Climate Data Center \(CDC\) \(2018\)](#) provided the 2 m surface temperature observations for a time range between January 2, 2015 to December 31, 2020, which leads to 2191 observation days over the six years. The observations will be denoted by Y_j , where the indices $j \in \{1, 2, 3, 4, 5\}$ refer to the lead times 24 h, 48 h, 72 h, 96 h, 120 h, respectively. Additionally, we reduced the $m = 50$ member forecast ensemble $\mathbf{X}_j := (X_j^{(1)}, \dots, X_j^{(m)})$ to its mean and standard deviation

$$\bar{X}_j := \frac{1}{m} \sum_{i=1}^m X_j^{(i)}, \quad S_j := \sqrt{\frac{1}{m-1} \sum_{i=1}^m (\bar{X}_j - X_j^{(i)})^2}, \quad (4.1)$$

for $j \in \{1, 2, 3, 4, 5\}$, respectively. To take account of seasonal variations, we make use of the forecast initialization day of the year, denoted by $X_{\text{doy}} \in \{1, 2, \dots, 366\}$. To capture

the dependence among the different lead times, we calculated the correlation $\text{Cor}(\mathbf{X}_i, \mathbf{X}_j)$ among the forecast ensembles for each lead time combination $i, j \in \{1, 2, 3, 4, 5\}$ with $i < j$. Note, that the realizations of the considered variables will be indicated by lowercase letters. Eventually, we use the period of 2015-2019 as training data set and the remaining days in 2020 as validation data set. The data is part of the data set by [Jobst et al. \(2023\)](#).

4.2 Methods

As already indicated, we follow the IFM approach for the multivariate postprocessing of 2m surface temperature of different lead times. Therefore, we firstly apply a univariate postprocessing method for each lead time separately and afterwards we restore the temporal dependencies via copula approaches.

4.2.1 Univariate Postprocessing

For the univariate postprocessing of 2m surface temperature forecasts, we make use of the ensemble model output statistics (EMOS) originally suggested by [Gneiting et al. \(2005\)](#). Specifically, we assume a normal distribution $Y_j \sim \mathcal{N}(\mu_j, \sigma_j^2)$ for the predictive distribution of each lead time case $j \in \{1, 2, 3, 4, 5\}$. Following [Lang et al. \(2020\)](#) and [Jobst et al. \(2024\)](#), we employ a smooth EMOS version, i.e. we assume

$$\mu_j := a_{0,j} + f_{0,j} + (a_{1,j} + f_{1,j}) \cdot \bar{x}_j, \quad \log(\sigma_j) := b_{0,j} + g_{0,j} + (b_{1,j} + g_{1,j}) \cdot s_j, \quad (4.2)$$

with coefficients $a_{0,j}, a_{1,j}, b_{0,j}, b_{1,j} \in \mathbb{R}$, ensemble mean \bar{x}_j and standard deviation s_j for $j \in \{1, 2, 3, 4, 5\}$. Furthermore,

$$f_{k,j} := \alpha_{k,j,1} \sin\left(\frac{2\pi x_{\text{doy}}}{365.25}\right) + \alpha_{k,j,2} \cos\left(\frac{2\pi x_{\text{doy}}}{365.25}\right) + \alpha_{k,j,3} \sin\left(\frac{4\pi x_{\text{doy}}}{365.25}\right) + \alpha_{k,j,4} \cos\left(\frac{4\pi x_{\text{doy}}}{365.25}\right), \quad (4.3)$$

$$g_{k,j} := \beta_{k,j,1} \sin\left(\frac{2\pi x_{\text{doy}}}{365.25}\right) + \beta_{k,j,2} \cos\left(\frac{2\pi x_{\text{doy}}}{365.25}\right) + \beta_{k,j,3} \sin\left(\frac{4\pi x_{\text{doy}}}{365.25}\right) + \beta_{k,j,4} \cos\left(\frac{4\pi x_{\text{doy}}}{365.25}\right), \quad (4.4)$$

denote truncated Fourier series to model the cyclic seasonal behavior in the intercept and slope with coefficients $\alpha_{k,j,l}, \beta_{k,j,l} \in \mathbb{R}$ for $k = 0, 1, j = 1, 2, 3, 4, 5, l = 1, 2, 3, 4$. All coefficients are optimized via the continuous ranked probability score (CRPS, [Matheson and Winkler \(1976\)](#)) with the training data set as static training period for each lead time separately. For the model estimation we make use of the R-package `crch` by [Messner et al. \(2016\)](#).

4.2.2 Multivariate postprocessing

In a second step we re-obtain the temporal dependencies among the 5 different lead times via different copula approaches. For that, we denote the postprocessed marginal distribution functions by F_1, \dots, F_5 for the 5 different lead times and consider the temporally ordered random vector $F \sim (Y_1, \dots, Y_5)$. In the following, we briefly summarize two common multivariate postprocessing techniques and present the setting for the conditional vine copula approach.

Ensemble copula coupling. The ensemble copula coupling (ECC, Schefzik et al., 2013) is based on the assumption, that the raw ensemble forecasts can capture the true multivariate dependence structure. Given the postprocessed univariate marginal distributions F_1, \dots, F_5 , the method is based on two steps:

1. Draw a sample $\hat{x}_j^{(1)}, \dots, \hat{x}_j^{(m)}$ of the same size as the raw ensemble from each postprocessed distribution F_j for $j = 1, \dots, 5$, which will be arranged in ascending order.
2. Calculate the permutations $\boldsymbol{\pi}_j := (\pi_j(1), \dots, \pi_j(m))$ by the rank order structure of the raw ensemble $\pi_j(k) := \text{rank}(\hat{x}_j^{(k)})$ for $k = 1, \dots, m$ with ties resolved at random for each postprocessed distribution F_j . To obtain the ECC-corrected forecast ensemble, the sample from step 1 is reordered according to the permutation $\boldsymbol{\pi}_j$ via

$$\tilde{x}_j^{(k)} := \hat{x}_{\pi_j(k)}^{(k)}, \quad k = 1, \dots, m, \quad (4.5)$$

for each postprocessed distribution F_j for $j = 1, \dots, 5$.

Different procedures for the drawing the sample in step 1 have been considered (Schefzik et al., 2013; Hu et al., 2016). To ensure a fair comparison among the methods, we draw m random samples

$$\hat{x}_j^{(1)} := F_j^{-1}(u_1), \dots, \hat{x}_j^{(m)} := F_j^{-1}(u_m), \quad (4.6)$$

from independently, uniform distributed samples u_1, \dots, u_m on $(0,1)$ for $j = 1, \dots, 5$. The method is implemented by an own R-code.

Gaussian copula approach. For the Gaussian copula approach (GCA, Möller et al., 2013), we assume that the dependence among the probability integral transformed observations $u_j = F_j(y_j)$ for $j = 1, \dots, 5$ can be captured by a multivariate Gaussian copula, i.e.

$$C(u_1, \dots, u_5) = \Phi_5(\Phi^{-1}(u_1), \dots, \Phi^{-1}(u_5) \mid \boldsymbol{\Sigma}), \quad (4.7)$$

where $\Phi_5(\cdot \mid \boldsymbol{\Sigma})$ denotes the cumulative distribution function of a 5-dimensional normal distribution with mean zero, correlation matrix $\boldsymbol{\Sigma}$, and Φ^{-1} denoting the quantile function of the univariate standard normal distribution Φ . The GCA consists of the following four steps:

1. Latent standard Gaussian observations are calculated via

$$\tilde{y}_j := \Phi^{-1}(F_j(y_j)), \quad (4.8)$$

employing a set of past observations (here all available observations in the training data set) and the postprocessed marginal distributions F_j for all $j = 1, \dots, 5$.

2. A parametric (here empirical) 5×5 correlation matrix $\hat{\boldsymbol{\Sigma}}$ of the 5-dimensional normal distribution Φ_5 is estimated from the latent standard Gaussian observations in step 1.
3. Multivariate random samples $\mathbf{Z}_1, \dots, \mathbf{Z}_m$ are drawn from $\mathcal{N}_5(\mathbf{0}, \hat{\boldsymbol{\Sigma}})$.

4. In a last step, the GCA postprocessed forecast ensemble of the validation data set is calculated via

$$\tilde{x}_j^{(k)} := F_j^{-1}(\Phi(z_j^{(k)})), \quad k = 1, \dots, m, \quad (4.9)$$

of each postprocessed univariate distribution F_j for $j = 1, \dots, 5$.

Note, that combining a multivariate Gaussian copula with Gaussian marginal distributions is equal to a multivariate Gaussian distribution. The implementation of this method is based on the function `rmvnorm` of the R-package `Rfast` by [Papadakis et al. \(2021\)](#).

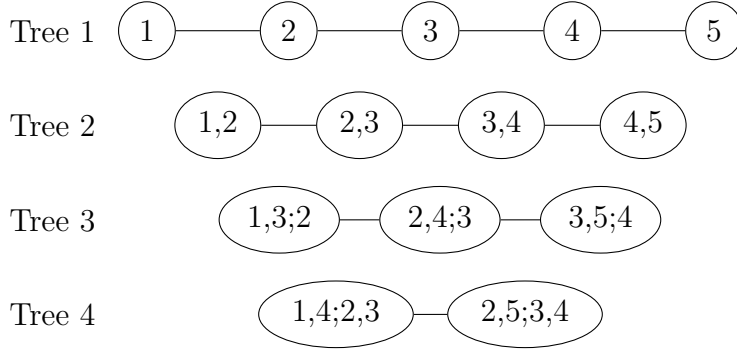


Figure 11: 5-dimensional D-vine.

Gradient-boosted conditional vine copula. For setting up a conditional vine copula, we first need to specify a regular vine. We choose a subclass, of a regular vine, called drawable vine (D-vine), where each node in each tree of the regular vine is connected at most to two other nodes (see Figure 11). As our data consists of a natural sequential ordering in the lead times $1 - 2 - 3 - 4 - 5$, a D-vine is particularly suited for this scenario (see, e.g. [Smith et al., 2010](#); [Nai Ruscone and Osmetti, 2016](#); [Czado, 2019](#)). For all conditional bivariate copulas we specify a GLM with the 15 covariates

$$\mathbf{Z} = \left(1, \left(\sin \left(\frac{2\pi k X_{\text{doy}}}{365.25} \right), \cos \left(\frac{2\pi k X_{\text{doy}}}{365.25} \right) \right)_{k=1,2}, (\text{Cor}(\mathbf{X}_i, \mathbf{X}_j))_{1 \leq i < j \leq 5} \right).$$

A seasonal varying intercept can be captured by the sine- and cosine transformed day of the year, while the correlations among the forecast ensembles of pair-wise different lead times are used to integrate information about the inter-temporal dependence. We estimate the conditional D-vine copula via gradient-boosting and covariate deselection (Algorithm 2). A maximum number of boosting iterations $m_{\text{stop}} = 500$, step length $\nu = 0.1$ and deselection threshold $\gamma = 0.01$ as in Section 3.2 turned out to be suited on the training data set. Furthermore, we specify two conditional vine copula models: one model (CVC) for which we allow all five copula families from the simulation study for each conditional bivariate copula and another model (CVC-G), where we select the Gaussian copula family for each conditional bivariate copula. In the latter case, the conditional D-vine copula corresponds to a conditional multivariate Gaussian copula ([Czado, 2019](#)) in contrast to GCA, where we employ an unconditional multivariate Gaussian copula. Note,

that the empirical correlation matrix of the observations shows with increasing lead time a reduction in the correlations, which reminds of a Toeplitz structure similar as employed in our simulation studies.

4.3 Verification methods

As we focus in this application on the verification of multivariate predictive distributions F , we make use of the *energy score* (ES, [Gneiting and Raftery, 2007](#)), which can be seen as an multivariate extension of the CRPS. Given a d -dimensional multivariate forecast F in terms of an m -member forecast ensemble $\mathbf{x}^{(1)}, \dots, \mathbf{x}^{(m)} \in \mathbb{R}^d$ and corresponding observation $\mathbf{y} = (y_1, \dots, y_d) \in \mathbb{R}^d$, the energy score is obtained by

$$\text{ES}(F, \mathbf{y}) = \frac{1}{m} \sum_{k=1}^m \|\mathbf{x}^{(k)} - \mathbf{y}\| - \frac{1}{2m^2} \sum_{k=1}^m \sum_{j=1}^m \|\mathbf{x}^{(k)} - \mathbf{x}^{(j)}\|, \quad (4.10)$$

where $\|\cdot\|$ denotes the Euclidean norm on \mathbb{R}^d . Furthermore, if F is given as multivariate forecast distribution function, the energy score can be obtain by the Monte-Carlo approximation

$$\text{ES}(F, \mathbf{y}) = \frac{1}{m} \sum_{k=1}^m \|\mathbf{x}^{(k)} - \mathbf{y}\| - \frac{1}{2(m-1)} \sum_{k=1}^{m-1} \|\mathbf{x}^{(k)} - \mathbf{x}^{(k+1)}\|, \quad (4.11)$$

where $\mathbf{x}^{(1)}, \dots, \mathbf{x}^{(m)}$ are samples issued from F ([Gneiting et al., 2008](#)). As it is advised to use multiple scores for assessing the predictive performance we additionally consider the *variogram score* of order p (VS^p , [Scheuerer and Hamill, 2015](#)) as a multivariate proper scoring rule. The score is defined as

$$\text{VS}^p(F, \mathbf{y}) = \sum_{i=1}^d \sum_{j=1}^d \omega_{ij} \left(|y_i - y_j| - \frac{1}{m} \sum_{k=1}^m |x_i^{(k)} - x_j^{(k)}|^p \right)^2, \quad (4.12)$$

where $\omega_{ij} \geq 0$ is the weight for pair (i, j) . Compared to other multivariate proper scoring rules, such as e.g. the energy score, the VS^p is more sensible to correlation misspecifications. We apply an unweighted version of the VS^p , i.e. $\omega_{ij} = 1$ for all pairs (i, j) with order $p = 0.5$ following the suggestions of [Scheuerer and Hamill \(2015\)](#). For the calculation of both scores, we choose a sample size of $m = 10000$ for a fair comparison among GCA, CVC and CVC-G, while we are by construction restricted to a sample size of $m = 50$ for the raw ensemble and ECC. Eventually, to assess the statistical improvements in terms of the considered scores, we conduct a Diebold-Mariano test ([Diebold and Mariano, 1995](#)) with automatic lag selection according to [Newey and West \(1994\)](#) and Bartlett weights for the heteroscedasticity and autocorrelation consistent variance estimator. We employ a significance level of $\alpha = 0.05$ for the following tests.

4.4 Results

Table 5 shows the mean scores of the raw ensemble as well as the ECC-, GCA-, CVC- and CVC-G-postprocessed ensemble forecasts in the validation data set. All postprocessing methods are able to considerably improve the raw ensemble with respect to $\text{VS}^{0.5}$ and

ES. Furthermore, CVC-G and CVC yield to significant improvements in terms of the considered scores over ECC and GCA. However, there are minor score differences among CVC-G and CVC suggesting, that the Gaussian dependence assumption is sufficient. The reduced forecast skill of CVC in comparison to CVC-G might be traced back to the slight overfitting in terms of the copula family selection (see also Figure 13). As we can already conclude from the $VS^{0.5}$ of CVC-G and CVC, conditionally modelling the temporal dependencies among the lead times can yield an improvement over models with constant dependence assumption such as GCA.

	Raw ensemble	ECC	GCA	CVC-G	CVC
$VS^{0.5}$	6.778 ^(0.055, 0.058)	6.695 ^(0.015, 0.016)	6.632 ^(0.002, 0.002)	6.587 ^(0.876)	6.589 ^(0.124)
ES	3.010 ^(0.000, 0.000)	2.784 ^(0.000, 0.000)	2.747 ^(0.040, 0.045)	2.744 ^(0.667)	2.744 ^(0.333)

Table 3: Verification scores aggregated over all time points in the validation data set. Bold values represent the best value for each score. The score exponents show the p -values in favor of the CVC-G (not underlined) and CVC (underlined) over the competing methods according to the Diebold-Mariano test.

In Figure 12, the monthly averaged differences between the correlation matrices of CVC-G and GCA are visualized. Roughly speaking, we observe clearly lower correlations (dark red) among the different lead time forecasts for CVC-G than for GCA in the summer and fall months. In contrast, there are overall smaller correlation differences in winter months among CVC-G and GCA. However, CVC-G yields for the same period also slightly higher correlations (light purple) among the forecasts of higher lead times than this is the case for GCA. These results indicate, that the correlation among the lead time forecasts changes over time and shows seasonal dependencies.

Figure 13 shows the predicted Kendall's τ correlation time series for each conditional bivariate copula depending on the tree level in the training data set. First of all, we can confirm the already detected seasonal patterns for Kendall's τ correlation induced by the seasonal intercept in the GLM. Interestingly, we observe higher correlations among the lead times in winter than in summer. This might be related to the fact, that the marginal distributions of all lead times show higher variances in winter and lower variances in summer as well lower mean in winter than in summer. Furthermore, forecasts with higher lead times exhibit higher Kendall's τ correlations amongst each other, and a higher variance in Kendall's τ correlations than forecasts with lower lead times. This is specifically pronounced in the first tree. Additionally, the seasonal effect in the Kendall's τ correlation time series and consequently its volatility reduces from tree level 1 to tree level 4. This is in line with our previous findings, that for the higher tree levels constant copula parameters might be sufficient. As the Kendall's τ correlations fluctuate mostly around zero for tree levels greater 2, truncating the conditional D-vine copula at tree level 2, i.e. assuming Independence copulas for all bivariate copulas after tree level 2 is a possible course of action. This approach yields only to small changes for CVC-G and CVC in terms of the considered scores (results not shown here).

The grids below each Kendall's τ time series in Figure 13 show the color-coded estimated coefficient of the covariates for each conditional bivariate copula in CVC. Covariate 1

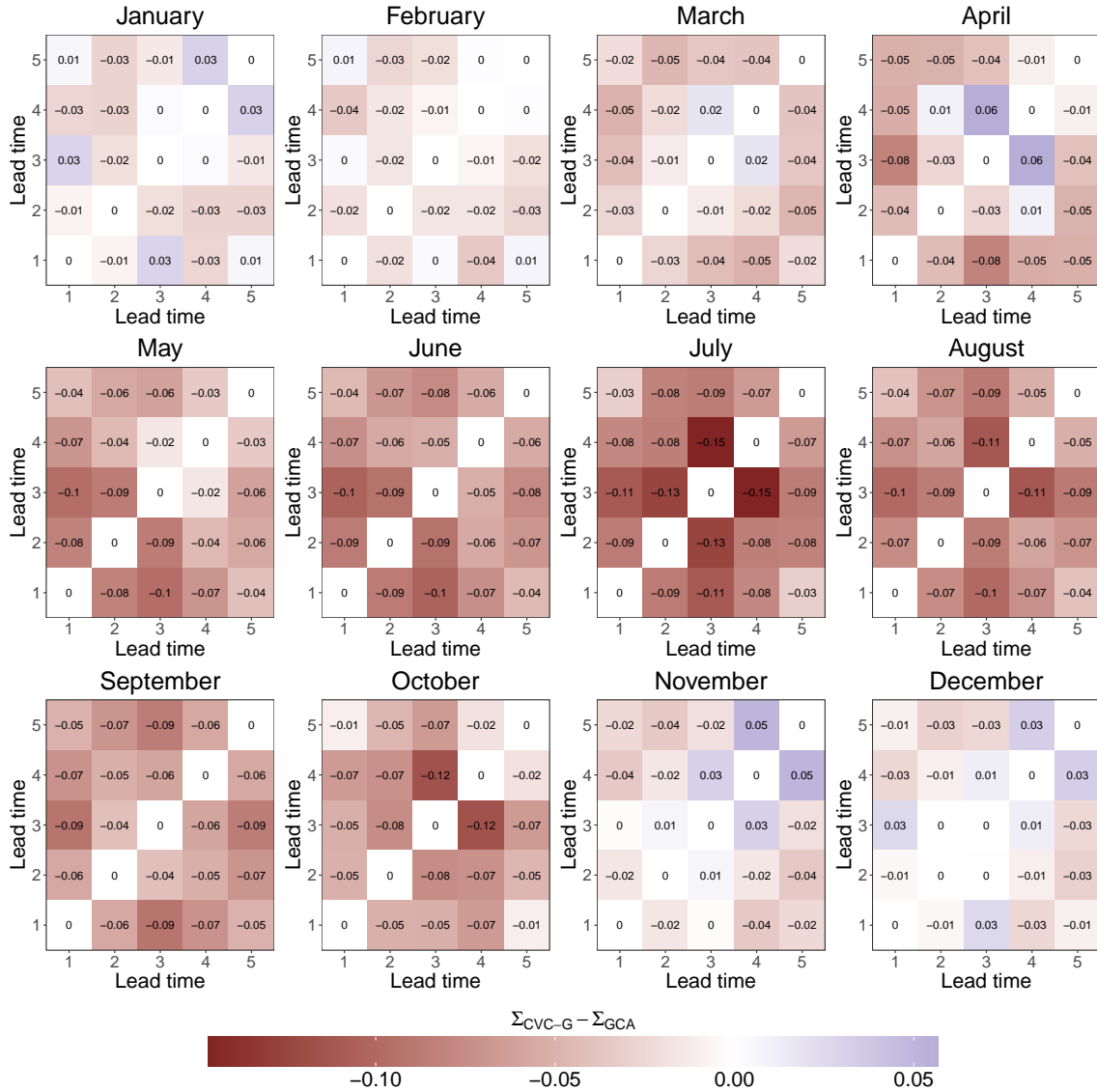


Figure 12: Monthly averaged differences between the correlation matrices of CVC-G and GCA in the validation data set.

represents the intercept and covariates $\sin 1$, $\cos 1$, $\sin 2$, $\cos 2$ correspond to the sine- and cosine transformed day of the year for order $k = 1, 2$, respectively. Additionally, e.g. covariate 25 corresponds to the correlation among the forecast ensemble \mathbf{X}_2 and \mathbf{X}_5 , i.e. $\text{Cor}(\mathbf{X}_2, \mathbf{X}_5)$. We observe that non-zero coefficients appear most frequently for tree level 1 and 2, which indicates that the dependence among the lead times can be influenced by covariates. As one may expect, copula 1,2 selects the corresponding lead time correlation-based covariate 12 in the first tree. Analogously, copula 2,3, copula 3,4 and copula 4,5 select its corresponding lead time correlation-based covariate 23, 34, 45, respectively. Additionally, its corresponding coefficient has a high value in contrast to the other coefficients, underlying its importance as predictor. In the second tree level, we can see that e.g. copula 3,5;4 selects the lead-time related covariate 35 but also covariates 15

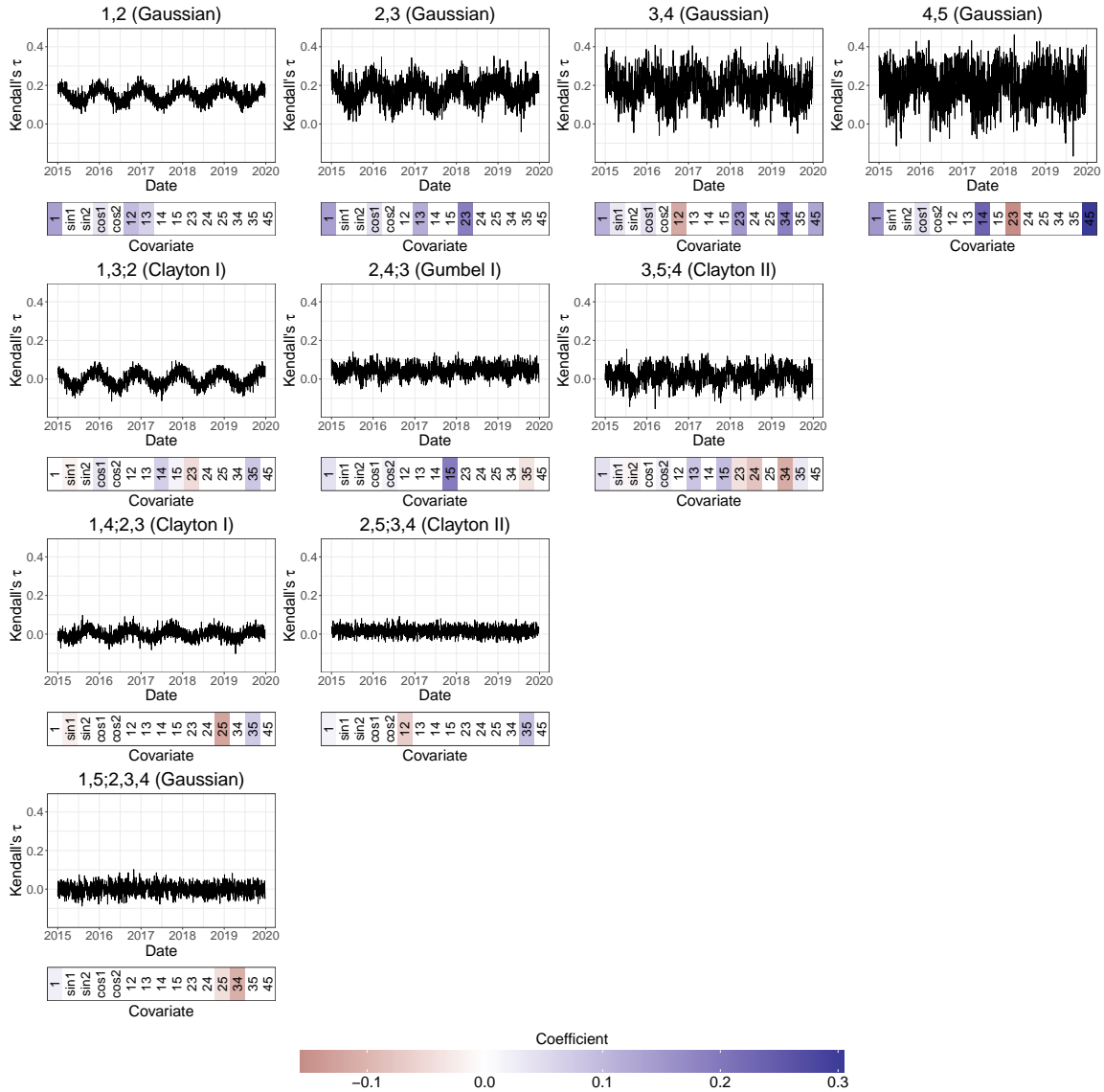


Figure 13: Kendall's τ correlation time series for each conditional bivariate copula (family) from tree level 1 (first row) to tree level 4 (last row) for CVC in the training data set. The corresponding color gradient indicates the value of the coefficient of the (selected) covariates for each conditional bivariate copula.

and 24 which might not be expected as predictors. Similar observations can be made for the other two copulas in the second tree level.

All in all, we conclude that CVC-G and CVC are able to significantly outperform state-of-the-art multivariate ensemble postprocessing methods and that a seasonally adaptive model for the temporal dependence among the lead time forecasts can considerably improve the predictive performance. However, explicitly linking the lead-time correlation-based covariates to the corresponding conditional bivariate copulas should be carefully considered.

5 Conclusion and outlook

In this work we introduced conditional vine copulas within a gradient-boosting estimation framework. Covariates are linked in terms of a GLM to the Kendall's τ correlation coefficient, from which the parameters for conditional bivariate copulas can be derived. The gradient-boosting Algorithm 2 allows a natural covariate selection and coefficient estimation adapted for sparse low- and high-dimensional covariate settings. Additionally, we extended the estimation procedure to conditional vine copulas.

In a simulation study we investigated a pre-specified GLM for 5 different bivariate copula families and for 5-dimensional conditional vine copulas in low- as well as high dimensional covariate settings. The results for the conditional bivariate copula fitting showed, that Algorithm 2 is able to detect the true effects and to select mostly the informative covariates in nearly each simulation scenario. Furthermore, AIC outperformed CV as stopping criterion and the AIC is suitable to identify the (true) copula family. For the estimation of the conditional vine copulas we observe, that the estimated effects are almost unbiased in the first two tree levels and that the (de)selection of (non-)informative covariates works well. Furthermore, increasing the sample size can provide more accurate fits. But there is an increasing shrinkage towards zero in the subsequent trees, which can yield to a biased copula family and covariate selection. However, this is a general issue for the estimation of conditional vine copulas already indicated by [Vatter and Nagler \(2018\)](#) and not only related to gradient-boosting.

In a case study for the lead time based postprocessing of 2 m surface temperature forecasts, CVC and CVC-G outperform benchmark methods in terms of variogram and energy score, indicating that the use of carefully selected covariates to predict the temporal dependencies can improve the multivariate performance. Besides of a promising forecast skill, CVC and CVC-G provided interesting insights in the covariate selection for the conditional bivariate copulas.

Despite of its merits, we detect some limitations of the conditional vine copulas in its current formulation. Firstly, our approach is not yet suited for discrete or mixed continuous-discrete responses. However, with slight modifications for the parameterization of the copula families, the gradient-boosting based estimation of conditional vine copulas can be extended based on the existing results for discrete ([Panagiotelis et al., 2012](#)) or mixed continuous-discrete ([Stöber, 2013](#)) responses. On top of our agenda is an extension of the conditional vine copulas in a gradient-boosting framework to the class of structured additive regression models (STAR, [Fahrmeir et al., 2021](#)). To reduce the increasing bias for the covariate effects in higher tree levels, we could first apply Algorithm 2 for the covariate selection. In a second step, the conditional bivariate copulas could be fitted on the reduced covariate set using the (penalized) maximum-likelihood estimation procedure by [Vatter and Nagler \(2018\)](#). Moreover, we only analyzed one-parametric copula families. However, the use of two-parametric copula families, such as e.g. Student- t copula where the second parameter depends on covariates as well would allow an even more flexible dependence modeling. To overcome this shortcoming, the work of [Thomas et al. \(2017\)](#) using a non-cyclic parameter updating with an adaptive step length ([Zhang et al., 2022](#)) in the gradient-boosting algorithm could be applied. Furthermore, in terms of non-sparse covariate scenarios, the cumulative risk suggested by [Strömer et al. \(2021\)](#) could be used in the R-package `boostCopula` to avoid a deselection of too many covariates. With regard

to applications, it would be interesting to conduct a more extensive comparison of our suggested method with other multivariate models in the field of ensemble postprocessing as well as for other applications.

Acknowledgements

We are grateful to the European Centre for Medium-Range Weather Forecasts (ECMWF) and the German Weather Service (DWD) for providing forecasts and observation data, respectively. Furthermore, the authors acknowledge support of the research by Deutsche Forschungsgemeinschaft (DFG) Grant Number 395388010. Annette Möller acknowledges support by Deutsche Forschungsgemeinschaft (DFG) Grant Number 520017589.

Appendix

A Conditional bivariate copulas

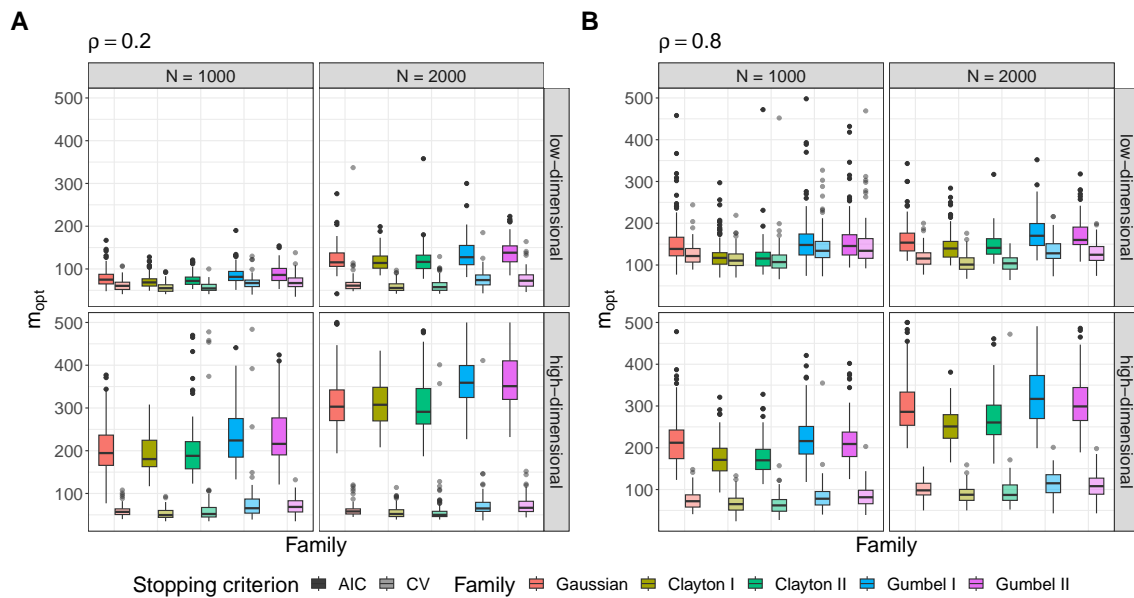


Figure 14: Optimal number of boosting iterations m_{opt} determined by AIC or CV for the low-correlated (A) and high-correlated (B) setting. The color represent the copula families while the color transparency stands for the stopping criterion.

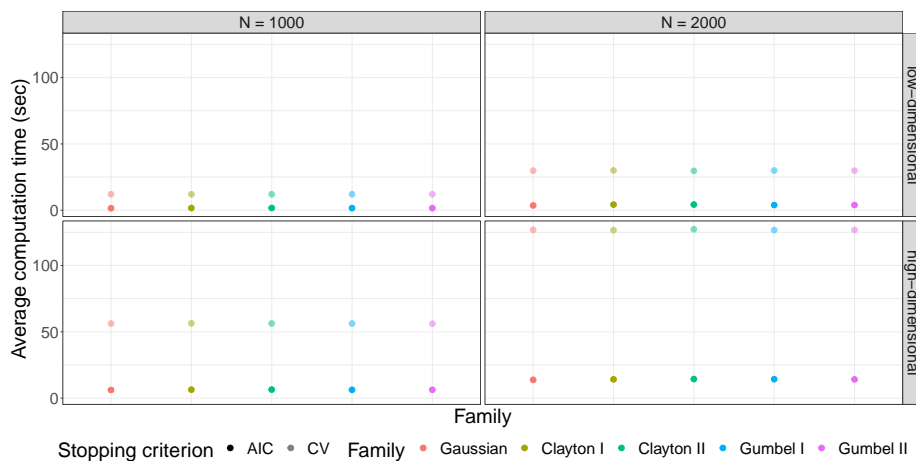


Figure 15: Computation times averaged over the the correlation settings $\rho \in \{0.2, 0.8\}$. The color represents the copula families while the color transparency stands for the stopping criterion.

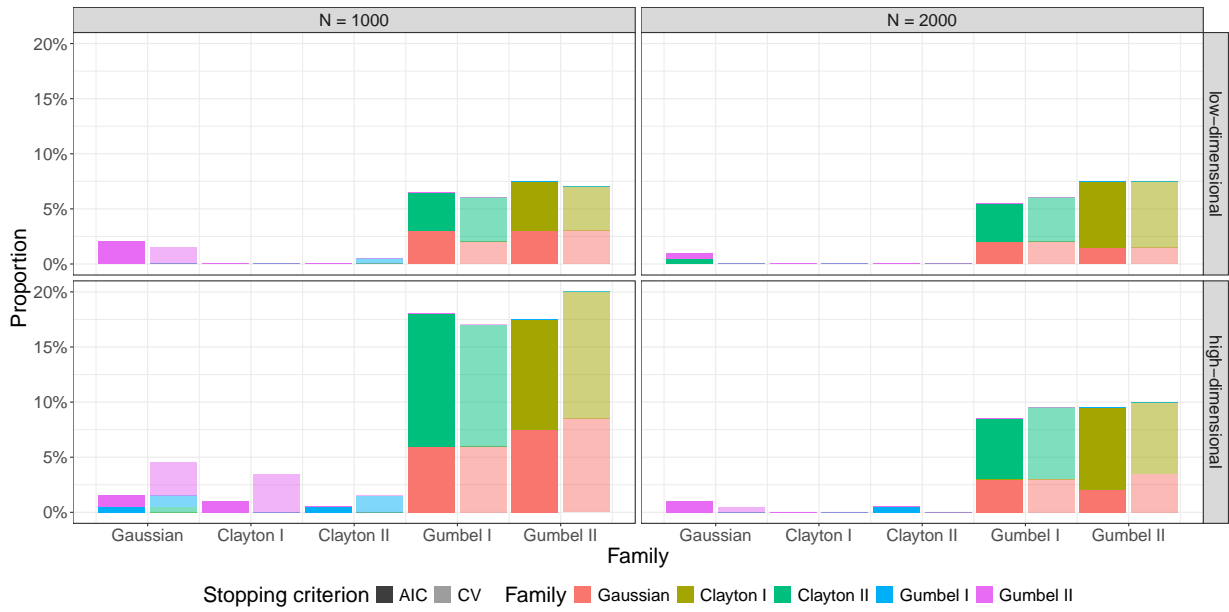


Figure 16: Percentage of false selected copula families for each specified copula family based on (in-sample) log-likelihood aggregated over the low-correlated and high-correlated setting. The color represents the copula families while the color transparency stands for the stopping criterion.

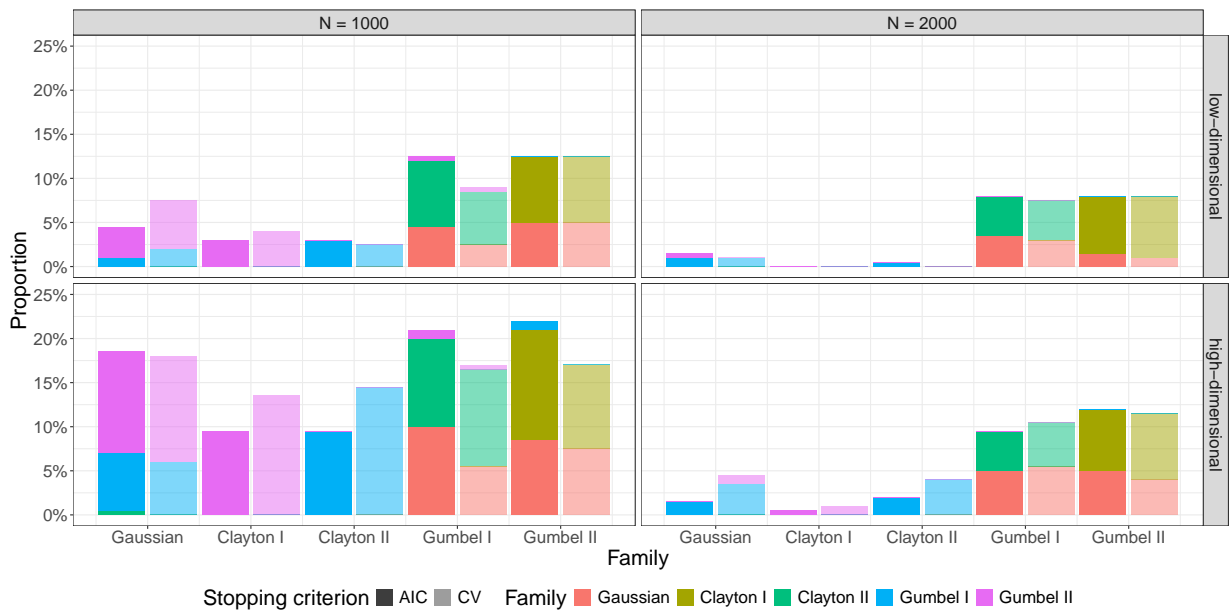


Figure 17: Percentage of false selected copula families for each specified copula family based on predictive risk using 25% of the training data for out-of-sample predictions aggregated over the low-correlated and high-correlated setting. The color represent the copula families while the color transparency stands for the stopping criterion.

B Conditional vine copulas

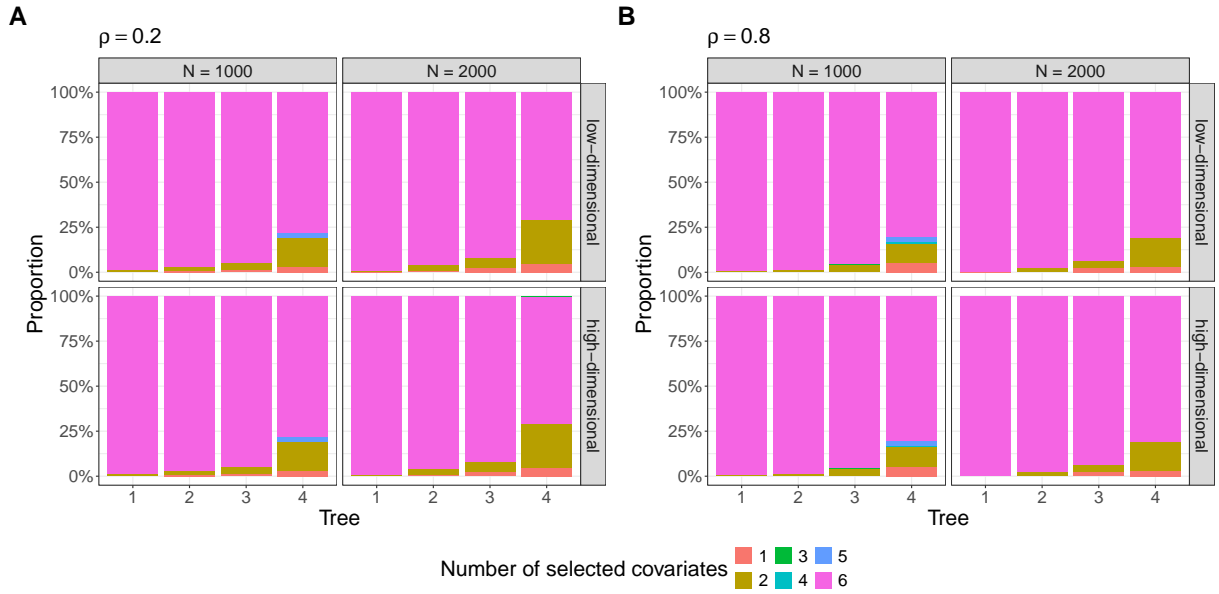


Figure 18: Bar charts for the proportion (%) of selected covariates across all copulas for each tree level and $n = 100$ repetitions in the “Specified” model for the low-correlated (A) and high-correlated (B) setting.

Model	Selected	Specified
low-dimensional	29	6
high-dimensional	106	11

Table 4: Mean computation times (in seconds) averaged over the correlation settings $\rho \in \{0.2, 0.8\}$ and sample sizes $N \in \{1000, 2000\}$.

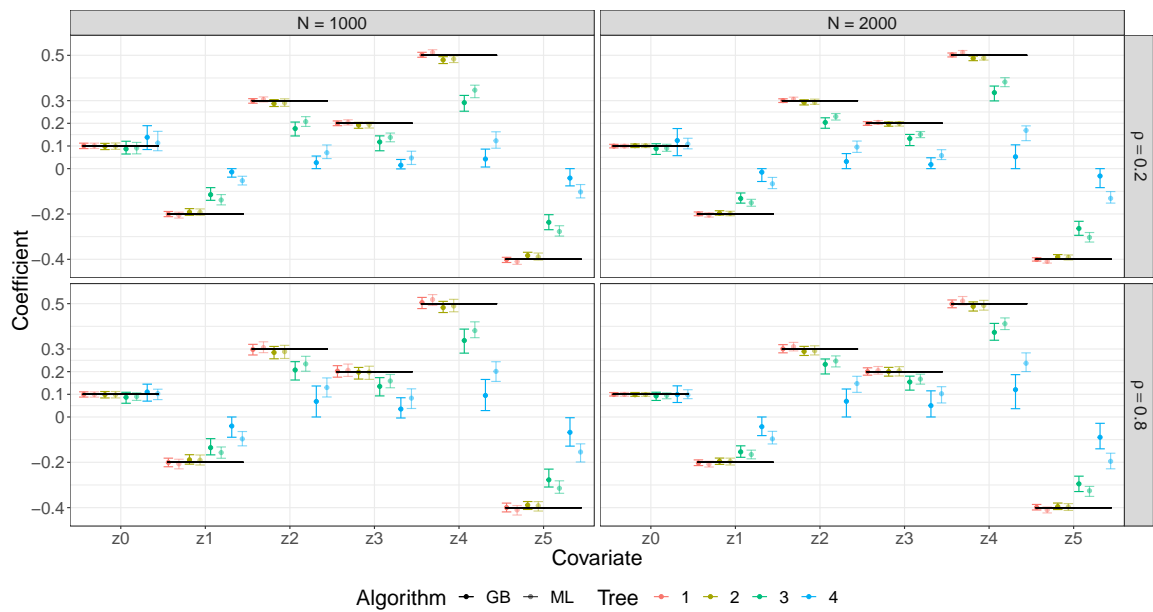


Figure 19: Summary of the estimated coefficients based on gradient-boosting (GB, Algorithm 1) and (penalized) maximum likelihood (ML, [Vatter and Chavez-Demoulin, 2015](#)). The copula families and the informative covariates have been selected in advance. The bars represent the interquartile range and the points denote the median of the estimated coefficients. The horizontal black lines correspond to the true coefficients. The color represent the tree level while the color transparency stands for the estimation algorithm.

C Application

Ziel and Berk (2019) propose the copula based variogram score (CVS^p) and energy score (CES) as an extension of existent multivariate scoring rules (see, e.g. Scheuerer and Hamill, 2015; Gneiting and Raftery, 2007). The copula based multivariate scoring rules allow to evaluate the forecast skill of the multivariate dependence independently of the marginal distributions. For more details on the definition of these scores and further information, we refer to Ziel and Berk (2019).

	Raw ensemble	ECC	GCA	CVC-G	CVC
$CVS^{0.5}$	0.964 ^(0.013, 0.012)	0.967 ^(0.004, 0.003)	0.956 ^(0.118, 0.122)	0.951 ^(0.539)	0.951 ^(0.0461)
CES	0.177 ^(0.000, 0.000)	0.178 ^(0.000, 0.000)	0.175 ^(0.276, 0.255)	0.175 ^(0.278)	0.175 ^(0.722)

Table 5: Copula based verification scores aggregated over all time points in the validation data set. Bold values represent the best value for each score. The score exponents show the p -values in favor of the CVC-G (not underlined) and CVC (underlined) over the competing methods according to the Diebold-Mariano test.

For assessing the calibration of multivariate forecasts, multivariate verification rank histograms (see, e.g. Gneiting et al., 2008; Thorarinsdottir et al., 2016) are frequently employed. We use in the following the multivariate ranking suggested by Gneiting et al. (2008), where we iteratively calculate the multivariate ranks of GCA, CVC-G and CVC for ensemble size $m = 50$ of all 10000 samples. The closer the distribution of the multivariate ranks to the discrete uniform distribution on $\{1, \dots, m + 1\}$ is, the better the calibration, where any deviation from uniformity indicates a lack of calibration. The deviation from uniformity can be further assessed by the reliability index (Monache et al., 2006), denoted by Δ , where a lower value represents a better calibration.

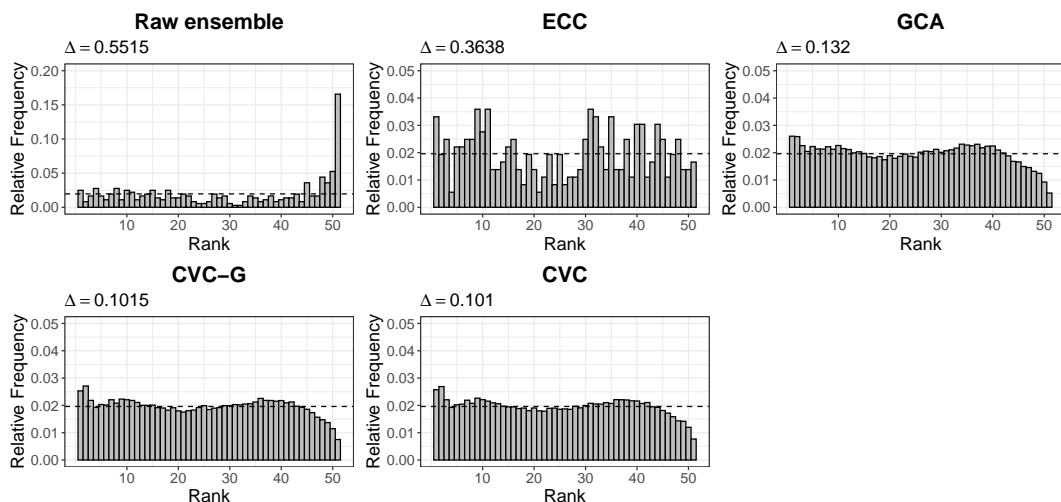


Figure 20: Multivariate verification rank histograms for the validation data set.

References

- Aas, K. et al. (2009). Pair-copula constructions of multiple dependence. In: 44, pp. 182–198. DOI: [10.1016/j.insmatheco.2007.02.001](https://doi.org/10.1016/j.insmatheco.2007.02.001).
- Acar, E. F., Craiu, R. V., and Yao, F. (2010). Dependence Calibration in Conditional Copulas: A Nonparametric Approach. In: *Biometrics* 67.2, pp. 445–453. DOI: [10.1111/j.1541-0420.2010.01472.x](https://doi.org/10.1111/j.1541-0420.2010.01472.x).
- Akaike, H. (1998). Information Theory and an Extension of the Maximum Likelihood Principle. In: *Springer Series in Statistics*. Springer New York, pp. 199–213. DOI: [10.1007/978-1-4612-1694-0_15](https://doi.org/10.1007/978-1-4612-1694-0_15).
- Bedford, T. and Cooke, R. M. (2001). Probability Density Decomposition for Conditionally Dependent Random Variables Modeled by Vines. In: *Annals of Mathematics and Artificial Intelligence* 32.1/4, pp. 245–268. DOI: [10.1023/a:1016725902970](https://doi.org/10.1023/a:1016725902970).
- Bedford, T. and Cooke, R. M. (2002). Vines—A New Graphical Model for Dependent Random Variables. In: *The Annals of Statistics* 30.4, pp. 1031–1068. DOI: [10.1214/aos/1031689016](https://doi.org/10.1214/aos/1031689016).
- Brechmann, E. C. (2010). Truncated and simplified regular vines and their applications. MA thesis. Technical University of Munich. URL: <https://mediatum.ub.tum.de/doc/1079285/1079285.pdf>.
- Bühlmann, P. and Hothorn, T. (Nov. 2007a). Boosting Algorithms: Regularization, Prediction and Model Fitting. In: *Statistical Science* 22.4. DOI: [10.1214/07-sts242](https://doi.org/10.1214/07-sts242).
- Bühlmann, P. and Hothorn, T. (2007b). Rejoinder: Boosting Algorithms: Regularization, Prediction and Model Fitting. In: *Statistical Science* 22.4. DOI: [10.1214/07-STSS242REJ](https://doi.org/10.1214/07-STSS242REJ).
- Bühlmann, P. and Yu, B. (2003). Boosting With the L_2 Loss. In: *Journal of the American Statistical Association* 98.462, pp. 324–339. DOI: [10.1198/016214503000125](https://doi.org/10.1198/016214503000125).
- Craiu, V. R. and Sabeti, A. (2012). In mixed company: Bayesian inference for bivariate conditional copula models with discrete and continuous outcomes. In: *Journal of Multivariate Analysis* 110, pp. 106–120. DOI: [10.1016/j.jmva.2012.03.010](https://doi.org/10.1016/j.jmva.2012.03.010).
- Czado, C. (2019). Analyzing Dependent Data with Vine Copulas. Springer International Publishing. DOI: [10.1007/978-3-030-13785-4](https://doi.org/10.1007/978-3-030-13785-4).
- Diebold, F. X. and Mariano, R. S. (1995). Comparing Predictive Accuracy. In: *Journal of Business & Economic Statistics* 13.3, pp. 253–263. DOI: [10.1080/07350015.1995.10524599](https://doi.org/10.1080/07350015.1995.10524599).
- Dißmann, J. et al. (2013). Selecting and estimating regular vine copulae and application to financial returns. In: *Computational Statistics & Data Analysis* 59, pp. 52–69. DOI: [10.1016/j.csda.2012.08.010](https://doi.org/10.1016/j.csda.2012.08.010).
- DWD Climate Data Center (CDC) (2018). Historische stündliche Stationsmessungen der Lufttemperatur und Luftfeuchte für Deutschland, Version v006. DWD Climate Data Center (CDC). URL: https://opendata.dwd.de/climate_environment/CDC/observations_germany/climate/hourly/air_temperature/historical/BESCHREIBUNG_obsgermany_climate_hourly_tu_historical_de.pdf.
- European Centre for Medium-Range Weather Forecasts (ECMWF) (2021). Gridded forecast. Creative Commons Attribution 4.0 International (CC BY 4.0). URL: <https://www.ecmwf.int>.

- Fahrmeir, L. et al. (2021). *Regression: Models, Methods and Applications*. Springer Berlin Heidelberg. DOI: [10.1007/978-3-662-63882-8](https://doi.org/10.1007/978-3-662-63882-8).
- Friedman, J. H. (2001). Greedy function approximation: A gradient boosting machine. In: *The Annals of Statistics* 29.5. DOI: [10.1214/aos/1013203451](https://doi.org/10.1214/aos/1013203451).
- Genest, C. et al. (2009). Editorial to the special issue on modeling and measurement of multivariate risk in insurance and finance. In: *Insurance: Mathematics and Economics* 44.2, pp. 143–145. DOI: [10.1016/j.insmatheco.2008.10.005](https://doi.org/10.1016/j.insmatheco.2008.10.005).
- Gijbels, I., Veraverbeke, N., and Omelka, M. (2011). Conditional copulas, association measures and their applications. In: *Computational Statistics & Data Analysis* 55.5, pp. 1919–1932. DOI: [10.1016/j.csda.2010.11.010](https://doi.org/10.1016/j.csda.2010.11.010).
- Gneiting, T. and Raftery, A. E. (2007). Strictly Proper Scoring Rules, Prediction, and Estimation. In: *Journal of the American Statistical Association* 102.477, pp. 359–378. DOI: [10.1198/016214506000001437](https://doi.org/10.1198/016214506000001437).
- Gneiting, T. et al. (2008). Assessing probabilistic forecasts of multivariate quantities, with an application to ensemble predictions of surface winds. In: *TEST* 17.2, pp. 211–235. DOI: [10.1007/s11749-008-0114-x](https://doi.org/10.1007/s11749-008-0114-x).
- Gneiting, T. et al. (2005). Calibrated Probabilistic Forecasting Using Ensemble Model Output Statistics and Minimum CRPS Estimation. In: *Monthly Weather Review* 133.5, pp. 1098–1118. DOI: [10.1175/mwr2904.1](https://doi.org/10.1175/mwr2904.1).
- Hans, N. et al. (2022). Boosting distributional copula regression. In: *Biometrics*. DOI: [10.1111/biom.13765](https://doi.org/10.1111/biom.13765).
- Hastie, T. and Tibshirani, R. (June 1990). *Generalized Additive Models*. Taylor & Francis.
- Hastie, T. (2007). Comment: Boosting Algorithms: Regularization, Prediction and Model Fitting. In: *Statistical Science* 22.4. DOI: [10.1214/07-sts242a](https://doi.org/10.1214/07-sts242a).
- Hastie, T. and Tibshirani, R. (1986). *Generalized Additive Models*. In: *Statistical Science* 1.3. DOI: [10.1214/ss/1177013604](https://doi.org/10.1214/ss/1177013604).
- Hofner, B., Mayr, A., and Schmid, M. (2016). gamboostLSS: An R Package for Model Building and Variable Selection in the GAMLSS Framework. In: *Journal of Statistical Software* 74.1. DOI: [10.18637/jss.v074.i01](https://doi.org/10.18637/jss.v074.i01).
- Hofner, B. et al. (2012). Model-based boosting in R: a hands-on tutorial using the R package mboost. In: *Computational Statistics* 29.1-2, pp. 3–35. DOI: [10.1007/s00180-012-0382-5](https://doi.org/10.1007/s00180-012-0382-5).
- Hu, Y. et al. (2016). A Stratified Sampling Approach for Improved Sampling from a Calibrated Ensemble Forecast Distribution. In: *Journal of Hydrometeorology* 17.9, pp. 2405–2417. DOI: [10.1175/jhm-d-15-0205.1](https://doi.org/10.1175/jhm-d-15-0205.1).
- Jobst, D., Möller, A., and Groß, J. (2023). Data set for the ensemble postprocessing of 2m surface temperature forecasts in Germany for five different lead times. Version 0.1.0. DOI: [10.5281/zenodo.8193645](https://doi.org/10.5281/zenodo.8193645). URL: <https://doi.org/10.5281/zenodo.8193645>.
- Jobst, D., Möller, A., and Groß, J. (2024). Time Series based Ensemble Model Output Statistics for Temperature Forecasts Postprocessing. In: DOI: [10.48550/ARXIV.2402.00555](https://doi.org/10.48550/ARXIV.2402.00555). arXiv: [2402.00555](https://arxiv.org/abs/2402.00555).
- Joe, H. (1996). Families of m -variate distributions with given margins and $m(m - 1)/2$ bivariate dependence parameters. In: *Institute of Mathematical Statistics Lecture Notes - Monograph Series*. Institute of Mathematical Statistics, pp. 120–141. DOI: [10.1214/lnms/1215452614](https://doi.org/10.1214/lnms/1215452614).

- Klein, N. and Kneib, T. (2015). Simultaneous inference in structured additive conditional copula regression models: a unifying Bayesian approach. In: *Statistics and Computing* 26.4, pp. 841–860. DOI: [10.1007/s11222-015-9573-6](https://doi.org/10.1007/s11222-015-9573-6).
- Lakatos, M. et al. (2023). Comparison of multivariate post-processing methods using global ECMWF ensemble forecasts. In: *Quarterly Journal of the Royal Meteorological Society* 149.752, pp. 856–877. DOI: [10.1002/qj.4436](https://doi.org/10.1002/qj.4436).
- Lang, M. N. et al. (2020). Remember the past: a comparison of time-adaptive training schemes for non-homogeneous regression. In: *Nonlinear Processes in Geophysics* 27.1, pp. 23–34. DOI: [10.5194/npg-27-23-2020](https://doi.org/10.5194/npg-27-23-2020).
- Marra, G. and Radice, R. (2017). Bivariate copula additive models for location, scale and shape. In: *Computational Statistics & Data Analysis* 112, pp. 99–113. DOI: [10.1016/j.csda.2017.03.004](https://doi.org/10.1016/j.csda.2017.03.004).
- Matheson, J. E. and Winkler, R. L. (1976). Scoring Rules for Continuous Probability Distributions. In: *Management Science* 22.10, pp. 1087–1096. DOI: [10.1287/mnsc.22.10.1087](https://doi.org/10.1287/mnsc.22.10.1087).
- Mayr, A. and Hofner, B. (2018). Boosting for statistical modelling-A non-technical introduction. In: *Statistical Modelling* 18.3-4, pp. 365–384. DOI: [10.1177/1471082x17748086](https://doi.org/10.1177/1471082x17748086).
- McNeil, A., Frey, R., and Embrechts, P. (2005). Quantitative Risk Management. Princeton: Princeton University Press.
- Messner, J. W., Mayr, G. J., and Zeileis, A. (2016). Heteroscedastic Censored and Truncated Regression with crch. In: *The R Journal* 8.1, pp. 173–181. DOI: [10.32614/RJ-2016-012](https://doi.org/10.32614/RJ-2016-012). URL: <https://doi.org/10.32614/RJ-2016-012>.
- Möller, A., Lenkoski, A., and Thorarinsdottir, T. L. (2013). Multivariate probabilistic forecasting using ensemble Bayesian model averaging and copulas. In: *Quarterly Journal of the Royal Meteorological Society* 139.673, pp. 982–991. DOI: [10.1002/qj.2009](https://doi.org/10.1002/qj.2009).
- Monache, L. D. et al. (2006). Probabilistic aspects of meteorological and ozone regional ensemble forecasts. In: *Journal of Geophysical Research* 111.D24. DOI: [10.1029/2005jd006917](https://doi.org/10.1029/2005jd006917).
- Nai Ruscone, M. and Osmetti, S. A. (July 2016). Modelling the Dependence in Multivariate Longitudinal Data by Pair Copula Decomposition. In: *Soft Methods for Data Science*. Springer International Publishing, pp. 373–380. DOI: [10.1007/978-3-319-42972-4_46](https://doi.org/10.1007/978-3-319-42972-4_46).
- Nelder, J. A. and Wedderburn, R. W. M. (1972). Generalized Linear Models. In: *Journal of the Royal Statistical Society. Series A (General)* 135.3, p. 370. DOI: [10.2307/2344614](https://doi.org/10.2307/2344614).
- Newey, W. K. and West, K. D. (Oct. 1994). Automatic Lag Selection in Covariance Matrix Estimation. In: *The Review of Economic Studies* 61.4, pp. 631–653. DOI: [10.2307/2297912](https://doi.org/10.2307/2297912).
- Panagiotelis, A., Czado, C., and Joe, H. (2012). Pair Copula Constructions for Multivariate Discrete Data. In: *Journal of the American Statistical Association* 107.499, pp. 1063–1072. DOI: [10.1080/01621459.2012.682850](https://doi.org/10.1080/01621459.2012.682850).
- Papadakis, M. et al. (2021). Rfast: A Collection of Efficient and Extremely Fast R Functions. R package version 2.0.3. URL: <https://CRAN.R-project.org/package=Rfast>.
- Patton, A. J. (2002). Applications of Copula Theory in Financial Econometrics. PhD thesis. University of California.

- Pinson, P. and Girard, R. (2012). Evaluating the quality of scenarios of short-term wind power generation. In: *Applied Energy* 96, pp. 12–20. DOI: [10.1016/j.apenergy.2011.11.004](https://doi.org/10.1016/j.apenergy.2011.11.004).
- R Core Team (2020). R: A Language and Environment for Statistical Computing. R Foundation for Statistical Computing. Vienna, Austria. URL: <https://www.R-project.org/>.
- Radice, R., Marra, G., and Wojtyś, M. (2015). Copula regression spline models for binary outcomes. In: *Statistics and Computing* 26.5, pp. 981–995. DOI: [10.1007/s11222-015-9581-6](https://doi.org/10.1007/s11222-015-9581-6).
- Sabeti, A., Wei, M., and Craiu, R. V. (2014). Additive models for conditional copulas. In: *Stat* 3.1, pp. 300–312. DOI: [10.1002/sta4.64](https://doi.org/10.1002/sta4.64).
- Sanchez, G. B. et al. (Mar. 4, 2024). Boosting Distributional Copula Regression for Bivariate Binary, Discrete and Mixed Responses. In: DOI: [10.48550/ARXIV.2403.02194](https://doi.org/10.48550/ARXIV.2403.02194). arXiv: [2403.02194](https://arxiv.org/abs/2403.02194) [stat.ME].
- Schefzik, R., Thorarinsdottir, T. L., and Gneiting, T. (2013). Uncertainty Quantification in Complex Simulation Models Using Ensemble Copula Coupling. In: *Statistical Science* 28.4. DOI: [10.1214/13-sts443](https://doi.org/10.1214/13-sts443).
- Scheuerer, M. and Hamill, T. M. (2015). Variogram-Based Proper Scoring Rules for Probabilistic Forecasts of Multivariate Quantities. In: *Monthly Weather Review* 143.4, pp. 1321–1334. DOI: [10.1175/mwr-d-14-00269.1](https://doi.org/10.1175/mwr-d-14-00269.1).
- Sklar, A. (1959). Fonctions de Répartition à Dimensions et Leurs Marges. In: *Publications de L’Institut de Statistique de L’Université de Paris* 8, pp. 229–231.
- Smith, M. et al. (Dec. 2010). Modeling Longitudinal Data Using a Pair-Copula Decomposition of Serial Dependence. In: *Journal of the American Statistical Association* 105.492, pp. 1467–1479. DOI: [10.1198/jasa.2010.tm09572](https://doi.org/10.1198/jasa.2010.tm09572).
- Stöber, J. (2013). Regular Vine Copulas with the simplifying assumption, time-variation, and mixed discrete and continuous margins. en. PhD thesis. Technische Universität München, p. 160. URL: <https://mediatum.ub.tum.de/1137287>.
- Stöber, J., Joe, H., and Czado, C. (2013). Simplified pair copula constructions—Limitations and extensions. In: *Journal of Multivariate Analysis* 119, pp. 101–118. DOI: [10.1016/j.jmva.2013.04.014](https://doi.org/10.1016/j.jmva.2013.04.014).
- Strömer, A. et al. (2021). Deselection of base-learners for statistical boosting—with an application to distributional regression. In: *Statistical Methods in Medical Research* 31.2, pp. 207–224. DOI: [10.1177/09622802211051088](https://doi.org/10.1177/09622802211051088).
- Thomas, J. et al. (2017). Gradient boosting for distributional regression: faster tuning and improved variable selection via noncyclical updates. In: *Statistics and Computing* 28.3, pp. 673–687. DOI: [10.1007/s11222-017-9754-6](https://doi.org/10.1007/s11222-017-9754-6).
- Thorarinsdottir, T. L., Scheuerer, M., and Heinz, C. (2016). Assessing the Calibration of High-Dimensional Ensemble Forecasts Using Rank Histograms. In: *Journal of Computational and Graphical Statistics* 25.1, pp. 105–122. DOI: [10.1080/10618600.2014.977447](https://doi.org/10.1080/10618600.2014.977447).
- Vannitsem, S., Wilks, D., and Messner, J. W. (2018). Statistical Postprocessing of Ensemble Forecasts. Elsevier. DOI: [10.1016/c2016-0-03244-8](https://doi.org/10.1016/c2016-0-03244-8).
- Vatter, T. and Chavez-Demoulin, V. (2015). Generalized additive models for conditional dependence structures. In: *Journal of Multivariate Analysis* 141, pp. 147–167. DOI: [10.1016/j.jmva.2015.07.003](https://doi.org/10.1016/j.jmva.2015.07.003).

- Vatter, T. and Nagler, T. (2018). Generalized Additive Models for Pair-Copula Constructions. In: *Journal of Computational and Graphical Statistics* 27.4, pp. 715–727. DOI: [10.1080/10618600.2018.1451338](https://doi.org/10.1080/10618600.2018.1451338).
- Veraverbeke, N., Omelka, M., and Gijbels, I. (2011). Estimation of a Conditional Copula and Association Measures. In: *Scandinavian Journal of Statistics* 38.4, pp. 766–780. DOI: [10.1111/j.1467-9469.2011.00744.x](https://doi.org/10.1111/j.1467-9469.2011.00744.x).
- Wood, S. N. (2017). *Generalized Additive Models*. Chapman and Hall/CRC. DOI: [10.1201/9781315370279](https://doi.org/10.1201/9781315370279).
- Zhang, B. et al. (Jan. 2022). Adaptive step-length selection in gradient boosting for Gaussian location and scale models. In: *Computational Statistics* 37.5, pp. 2295–2332. DOI: [10.1007/s00180-022-01199-3](https://doi.org/10.1007/s00180-022-01199-3).
- Ziel, F. and Berk, K. (Oct. 2019). Multivariate Forecasting Evaluation: On Sensitive and Strictly Proper Scoring Rules. In: arXiv: [1910.07325](https://arxiv.org/abs/1910.07325) [[stat.ME](https://arxiv.org/abs/1910.07325)].